DMOCRATIC AND POPULAR REPUBLIC OF ALGERIA
MINISTRY OF HIGHER EDUCATION AND SCIENTIFIC RESEARCH
DJILALI BOUNAAMA UNIVERSITY OF KHEMIS MILIANA

Faculty of Science and Technology

Department of Technology

Dissertation Submitted for a Master's Degree in Mechanical Engineering

Speciality: Mechanical Construction

Design and Construction of SCARA Type Manipulator Robot Using CATIA V5 and Controlled With ARDUINO

Presented by:

Bardad Salah-Eddine

Bourorga Abderrahmane

Supervised by:

Dr. Bendali Nadir

Jury Members:

- **President :** Dr. Abbadeni.M
- **Examiner:** Dr. Belahcene.M

Academic Year: 2022/2023


بسم الله الرحمن الرحيم

ACKNOWLEDGMENTS

First of all, we would like to thank ALLAH for having given us the physical strength and mental power to accomplish this work.

We are greatly indebted to our thesis supervisor Dr, BENDALI.N for kindly providing guidance and interest throughout the development of this study. We would like to thank the members of the jury for their presence, for their attentive reading of our thesis as well as for the comments they have given us in order to improve our work. We would like to express our gratitude to all the teachers who have contributed to our university education.

Also we would like to thank Hydro-Industrie Company for letting us use their machines. I also thank Mr, BOULAGH.F for helping us a lot by giving us valuable advice and ideas.

Finally, we thank all those who have contributed directly or indirectly to the development of this modest work, find here the expression of our deep gratitude and respect.

ملخص

أي نظام آلي له علاقة بين الميكانيكا والإلكترونيا، والتي تتحقق من خلال دراسة المشغلات والسلاسل الحركية المرتبطة بها. في هذا المشروع ، يتم تقديم منهجية لتصميم وبناء روبوت مناور من نوع SCARA تتضمن العملية الإدراك من خلال الدراسة الحركية والديناميكية لسلسلة الروبوت SCARA مع اربعة درجات حرية، إلى جانب تصميم وتنفيذ محاكاة حركية باستخدام برنامج CATIA V5 . وفي الاخير نقوم تصنيع أجزاء SCARA وتجميعها والتحكم فيها باستخدام لوحة Arduino.

الكلمات المفتاحية: روبوت SCARA؛ برنامج CATIA V5؛ النمذجة الرياضية؛ محاكاة؛ اردوينو.

ABSTRACT

Any robotic system has a relationship between mechanics and electronics, which is materialized by the study of actuators and associated kinematic chains. In this project, a methodology for designing and constructing a manipulator robot of type SCARA is presented. The process involves the realization with kinematic and dynamic study of the robot Series SCARA with 4DOF, along with designing and performing a kinematic simulation using CATIA V5 software. Finally we manufacturing the parts of the SCARA, assembling and controlling them using an Arduino board.

Keywords: SCARA Robot; CATIA V5; Mathematical modelling; Simulation; Arduino.

RÉSUMÉ

Tout système robotique présente une relation entre la mécanique et l'électronique, qui se matérialise par l'étude des actionneurs et des chaînes cinématiques associées. Dans ce projet, une méthodologie de conception et de construction d'un robot manipulateur de type SCARA est présentée. Le processus implique la réalisation d'une étude cinématique et dynamique de la série de robots SCARA à 4DOF, ainsi que la conception et la réalisation d'une simulation cinématique à l'aide du logiciel CATIA V5. Enfin, nous fabriquons les pièces du SCARA, les assemblons et les contrôlons à l'aide d'une carte Arduino.

Mots-clés: Robot SCARA; CATIA V5; Modélisation mathématique; Simulation; Arduino.

CONTENTS

LIST OF ABBREVIATIONS

DOF	Degrees Of Freedom
SCARA	Selective Compliance Articulated Robot Arm
CAD	Computer-aided design
CAM	Computer-Aided Manufacturing
CAE	Computer-Aided Engineering
CATIA	Computer Aided Three-Dimensional Interactive Application
PUMA	Programmable Universal Machine for Assembly
A.F.N.O.R	French Association for Standardisation
A.M.S	Additional Member System
IFR	International Federation of Robotics
DGM	The Direct Geometric Model
RRPR	Rotation, Rotation, Prismatic and Rotation
DH	DENAVET- HARTENBERG
3D	Three-Dimensional
J	The jacobian
C	Cosinus
S	Sinus
θ	Degree of rotation
$\dot{q}$	the joint velocities
RC	Radio Control
IC	Integrated Circuit
PCB	printed circuit board
PWM	Pulse Width Modulation
USB	Universal Serial Bus
ICSP	In-Circuit Serial Programming
AC	Alternating Current
DC	Direct Current

MCU	Mecrocontroller unit
Tx/Rx	Transmit/Receive data
IDE	Integrated Development Environment
GPS	The Global Positioning System
d	Distance between the arm and organ terminal
a	Length of arm
V	Speed
m	The mass

LIST OF FIGURS

LIST OF TABLES

GENERAL INTRODUCTION

General introduction:

Over the past few decades, robots have attracted great interest in scientific research and engineering applications. Many efforts have been made in robotics, so different types of robots have been developed and studied [1].

The primary reason for using a robotic manipulator is to reduce human effort. These robotic manipulators are famous for the processing speed, control, precision, and accuracy of pick and place activities required in assembly line operations. The Selective Compliance Assembly Robotic Arm (SCARA) usually has 4DOF (Degrees Of Freedom), one linear, and three rotational motions [2]. The study proceeds according to the following five steps: model the robot by creating mathematical models: geometric, kinematic, and dynamic, then design the model of the robot with CAD software, then simulate the operation of the robot, and then simulate the control of the motors of the robot, and finally, realize and verify the operation of the robot[4].

This project deals with designing a manipulator robot of type SCARA followed by a realization with kinematic and dynamic study of this poly-articulated system. To obtain the geometrical parameters of this simple open chain mechanism, we present a dimensional and kinematic modeling of the chosen structure, and this step remains a critical task since the performance criteria of a given architecture depend very strongly on the dynamic model. Finally, we present the different steps of realization of the SCARA manipulator robot with a 3D model realized with the help of CATIA V5 software and controlled with ARDUINO

This study has been organized into three chapters:

- The first chapter provides general information about the field of robotics and its applications.
- The second chapter presents the mathematical models used to describe the motion of the robot joints: geometric, kinematic and dynamic. Then, the target robot's modelling, design and simulation will be described in detail.
- The last chapter will present the process of realization of the electronic and mechanical systems.

CHAPITRE I:

LITERATURE ON ROBOTICS

I.1 Introduction

The widespread use of robot manipulators in the current stage of industrial development has led to productivity improvements and improved quality of manufactured products, mainly due to the more excellent repeatability of robot movements, which has consequently led to greater accuracy in their performance. Although the first applications of such manipulators appeared in the painting and welding processes, the automotive industry soon began to use them, expanding their scope to handle bodies, engines, chassis, and other components [4].

This chapter aims to give a comprehensive account of robotics, including a brief historical background on the evolution of industrial robots, a broad categorization of robotics, and an overview of its constituent components.

I.2 History:

- 1920: Czech playwright Karel Capek introduced the word "robot" in his 1920 play Rossum's Universal Robots. The word "Robota" in Czech means "work". Despite these practical beginnings, science fiction writers and early Hollywood films gave us a romantic notion of robots. The anthropomorphic nature of these machines has introduced the notion of a robot, an element of man's search for his own identity [5].

- 1961: Unimation, the first industrial robot, emerged as a direct evolution of remote manipulators initially designed for the nuclear industry. George Devol and Joseph Engelberg founded the American company Unimation (now known as Staubi Unimation), which marketed this robot. General Motors was the first to utilize it on its assembly lines. With a weight of 1.5 tons, this robot could manipulate castings weighing up to 150 kg. [6]

- 1972: Nissan inaugurated the world's first fully robotized production line.

- 1978: General Motors developed the PUMA (Universal Programmable Machine for Assembly), which is still being used today. [3]

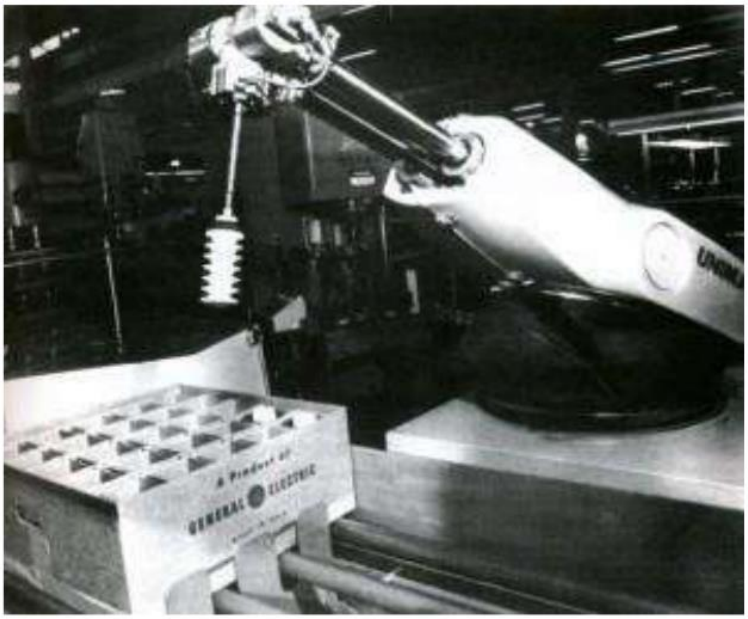

Figure I. 1: Robot Unimate [3].

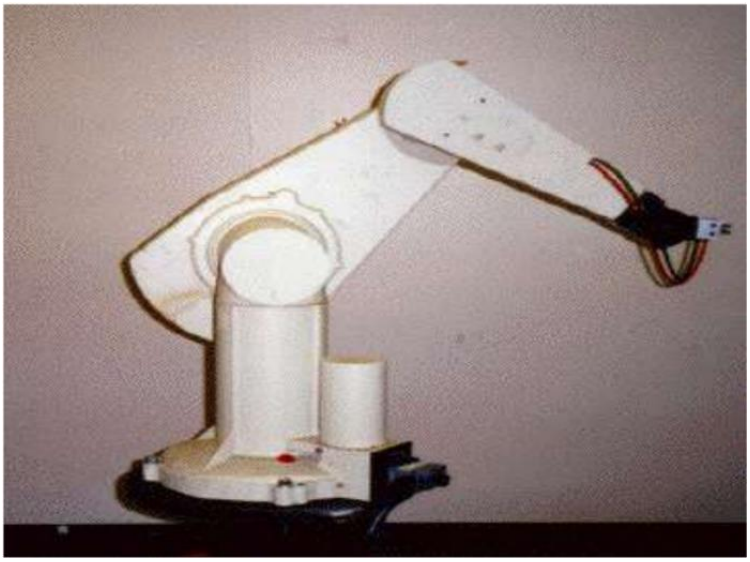

Figure I. 2: Robot Puma [3].

- 1947: first remotely operated electric manipulator.

- 1954: first programmable robot.

- 1961: the first robot with force control.

- 1963: use of vision to control a robot.

I.3 Definition

I.3.1 The robotics:

The origins of robotics can be traced back to deep cultural roots spanning centuries. Humans have always sought substitutes that could mimic their behaviour in various interactions with the environment. This constant search has been driven by diverse motivations, including philosophical, economic, social, and scientific principles. However, in the 1940s, Russian author Isaac Asimov envisioned robots as mechanical beings with human-like appearances but without emotions. These robots were controlled by a "positronic" brain programmed to adhere to ethical rules set by humans. Asimov coined the term "robotics" as the study of robots based on three fundamental laws.

1. A robot cannot harm a human being or allow a human being to be harmed through inaction.
2. A robot must obey human orders, except if such orders conflict with the first law.
3. A robot must protect its own existence as long as such protection does not conflict with the first or second law. These laws serve as the foundation of the field of robotics and are intended to guide the ethical development and use of robots.

Asimov's laws established guidelines for designing robots, which have since become an industrial products created by engineers and technicians. From a scientific perspective, a robot is a machine capable of modifying its environment through actions that follow specific rules and are influenced by acquired data. Robotics is the study of the intelligent connection between perception and action. A robotic system is a complex structure consisting of multiple subsystems, such as a mechanical system with a locomotion and manipulation apparatus. For example, the system may include two mechanical arms a mobile vehicle carries [7], as shown in **Figure 3**.

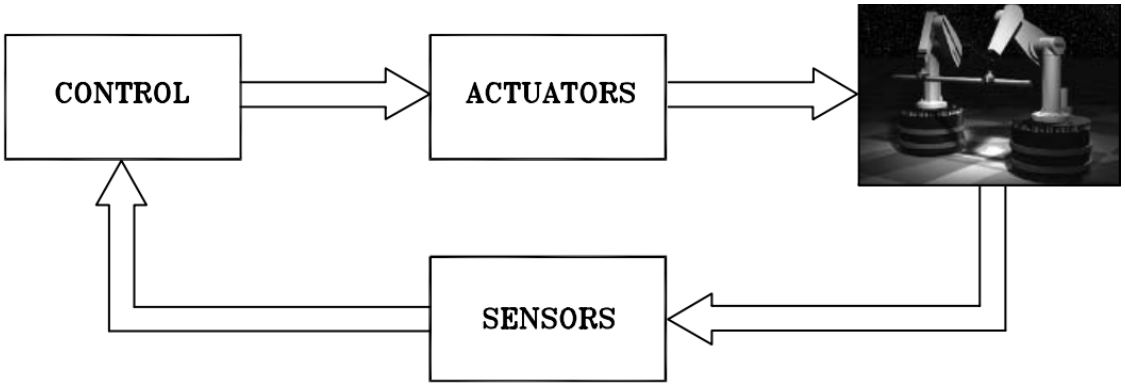

Figure I. 3: Components of a robotic system [7].

I.3.2 Robot:

- A robot is a complex mechanical system comprising multiple articulated parts powered by actuators and a computer. Its purpose is to carry out a diverse range of tasks.

- An automatic device that can manipulate objects and perform tasks based on a programmable set of instructions that can be modified or adapted as needed.

- A robot is an automatic system with an articulated mechanical structure as its operative part.

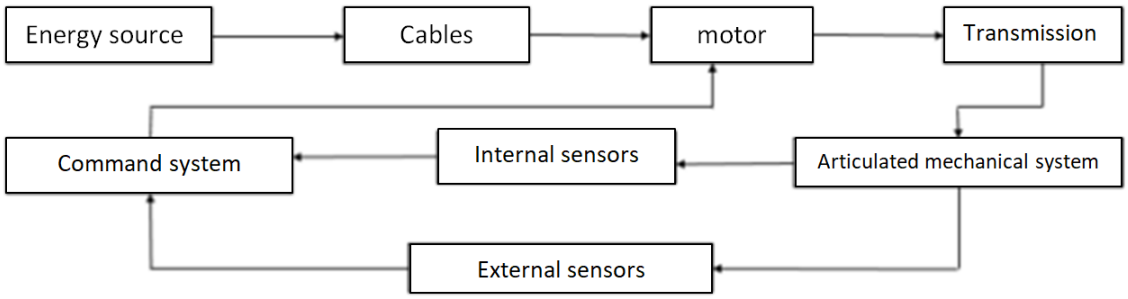

Figure I. 4: Command-control and operational parts of a robot [6].

To “deserve” the name of the robot, a system must have a certain flexibility Characterized by the following properties:

- Versatility: A robot must have the ability to perform a variety of Tasks or the same Task in different ways;

- Self-adaptability: A robot must be able to adapt to a changing environment during the execution of its tasks.

- The French Association for Standardization (A.F.N.O.R) defines a robot as a mechanical system of the manipulator type controlled in position, reprogrammable, versatile (i.e., multiple uses), with several degrees of freedom, capable of manipulating objects.

Materials, parts, tools, and specialized devices, in variable and programmed movements for the performance of a variety of tasks [4].

I.4 Components of a robot:

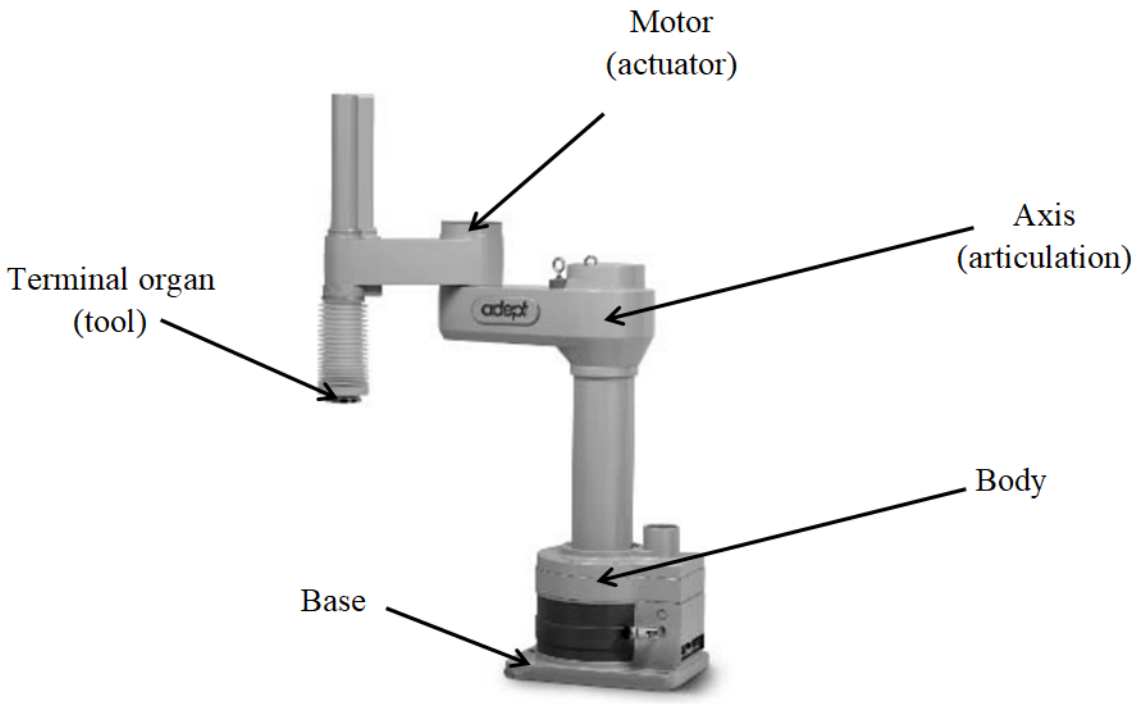

Figure I. 5: The AdeptOne XL robot (cortesy of Adept Technology Inc) [7].

I.4.1 The terminal organ:

The end effector, also called the terminal organ, encompasses all devices designed to manipulate or transform objects, including clamping devices, magnetic devices, vacuum devices, tools, welding torches, paint guns, Etc. These devices enable

the robot to interact with its environment effectively. Moreover, an end effector can be multifunctional and equipped with various devices for different purposes [3].

I.4.2 The articulated mechanical system (A.M.S):

The A.M.S. has a structure that closely resembles the human arm. Its purpose is to replace or extend human actions, and it should not be confused with autonomous mobile robots. The A.M.S. is a manipulator designed to position and orient its terminal device with specific speed and acceleration characteristics. It consists of a kinematic chain of bodies that are typically rigid and connected by articulations. The A.M.S. is motorized by electric, pneumatic, or hydraulic actuators, which transmit their movements to the joints through appropriate systems [6].

I.4.3 Articulations (joint)

In robotics, a joint connects two consecutive bodies while restricting the range of motion of one relative to the other. A joint's mobility degree is denoted by m, where $1< m \leq 6$.

A joint is considered simple when m = 1, the most prevalent type of joint in robotics. These simple joints can be either rotoid or prismatic [4]

I.4.4 The control part:

To control the robot's movements, the servocontrols that operate the actuators are directed by the control module. This module synthesizes the setpoints for the servocontrols by utilizing information from the perception function as well as user input. Additionally, the man-machine interface provides a means for users to program the robot's tasks and operations, further enabling precise control over the robot's actions [6].

I.5 Classification of robots

Robots can be classified according to their degrees of freedom, motion characteristics, kinematic structure, drive technology and geometry workspace [8].

I.5.1 Degree of freedom

In the context of mechanics, degrees of freedom refers to the specific and defined modes in which a mechanical system or device can move. The degrees of freedom are equivalent to the total number of independent displacements or aspects of motion. Even if a machine operates in two or three dimensions, it may have more than three degrees of freedom. The term is commonly used to describe the motion capabilities of robots. For instance, let us take a robot arm designed to mimic a human arm. Shoulder motion can occur as pitch (up and down) or yaw (left and right). Elbow motion can only occur as pitch. Wrist motion can occur as pitch or yaw, and rotation (roll) may also be possible for the wrist and shoulder [8].

I.5.2 Workspace Geometry

The geometric workspace denotes the environment section the manipulator's end-effector can reach. The shape and size of the workspace are determined by the manipulator's structure, as well as the existence of mechanical joint limits.

The objective of the robot arm is to position the wrist, which, in turn, will orient the end-effector. The classification of manipulators as Cartesian, cylindrical, spherical, SCARA, and anthropomorphic is based on the kind and sequence of the arm's degrees of freedom, beginning from the base joint [7].

I.5.2.1 Cartesian geometry

With three prismatic links, this structure is the oldest historically. It is logically derived from the traditional design of a three-axis machine tool, such as a milling or grinding machine. However, this structure is relatively uncommon, except in a few specific applications such as practical robots, shopping robots, etc [9].

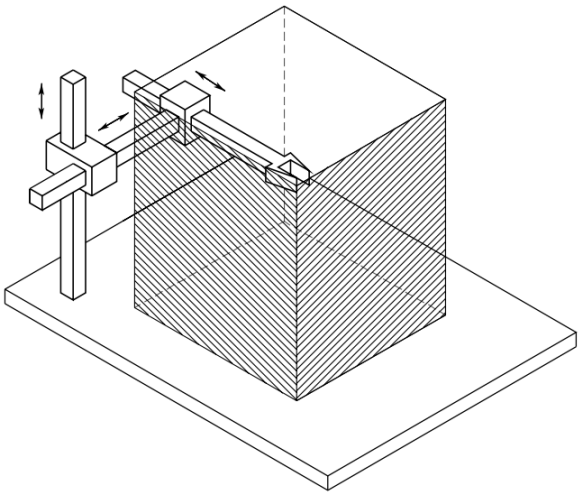

Figure I. 6: Cartesian manipulator and its workspace [7].

I.5.2.2 Cylindrical geometry

Cylindrical geometry differs from Cartesian geometry in that the first prismatic joint is replaced with a revolute joint (**Figure I.7**). If the task is described in cylindrical coordinates, then each degree of freedom corresponds to a Cartesian space variable as well. The cylindrical structure provides good mechanical stiffness, but the accuracy of wrist positioning decreases as the horizontal stroke increases. The workspace of a cylindrical manipulator is a section of a hollow cylinder (**Figure I.7**). The horizontal prismatic joint makes the wrist of a cylindrical manipulator well-suited for accessing horizontal cavities. Cylindrical manipulators are mainly used for carrying objects, even large ones, and in such cases, hydraulic motors are preferred over electric motors [7].

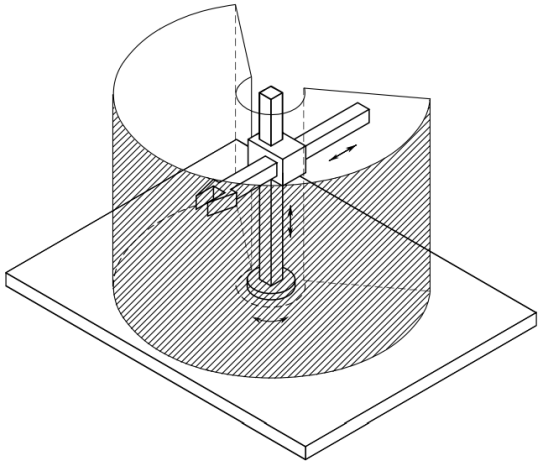

Figure I. 7: Cylindrical manipulator and its workspace [7].

I.5.2.3 Spherical geometry

Spherical geometry differs from cylindrical geometry in replacing the second prismatic joint with a revolute joint (**Figure I.8**). Each degree of freedom corresponds to a Cartesian space variable, provided the task is described in spherical coordinates. However, the mechanical stiffness of spherical manipulators is lower than that of the other two geometries, and the mechanical construction is more complex. Additionally, as the radial stroke increases, the wrist positioning accuracy decreases. The workspace of a spherical manipulator is a portion of a hollow sphere and it can also include the supporting base of the manipulator, thus allowing for the manipulation of objects on the floor. Spherical manipulators are primarily employed for machining, and electric motors are typically used to actuate the joints [7].

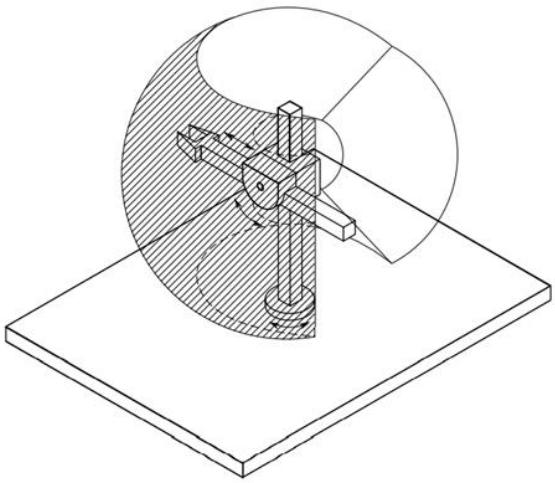

Figure I. 8: Spherical manipulator and its workspace [7].

I.5.2.4 SCARA geometry:

Another geometry commonly used in robotics is the SCARA (Selective Compliance Assembly Robot Arm) geometry, which is realized by placing two revolute joints and one prismatic joint in a configuration where all axes of motion are parallel. The SCARA structure offers high stiffness to vertical loads and compliance to horizontal loads, making it particularly well-suited to vertical assembly tasks. However, the correspondence between the degree of freedom and Cartesian space variables is only maintained for the vertical component of a task described in Cartesian coordinates. As the distance of the wrist from the first joint axis increases, the wrist positioning accuracy decreases. The typical workspace of a SCARA manipulator is illustrated in Figure 9, and it is well-suited for manipulating small objects. The joints of the SCARA manipulator are typically actuated by electric motors [7].

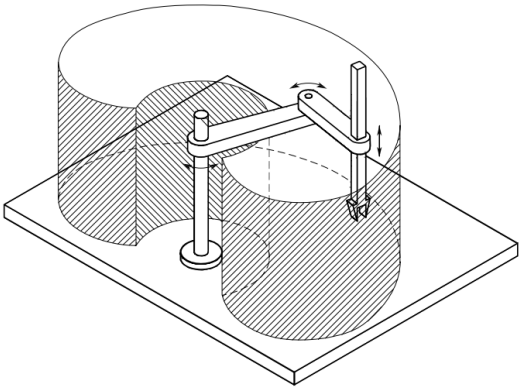

Figure I. 9: SCARA manipulator and its workspace [7].

I.5.2.5 Anthropomorphic geometry:

Anthropomorphic geometry in robotics is realized using three revolute joints, with the first joint's revolute axis being orthogonal to the axes of the other two joints, which are parallel (**Figure I.10**). The second and third joints are commonly referred to as the shoulder and elbow joints, respectively, given their similarity to the human arm. The anthropomorphic structure is the most dexterous geometry because all the joints are revolute, offering a greater range of motion. However, the correspondence between the degrees of freedom and Cartesian space variables is lost, and wrist positioning accuracy varies inside the workspace. The workspace of the anthropomorphic manipulator is

approximately a portion of a sphere, with a large volume compared to the manipulator's encumbrance. Electric motors typically actuate joints in anthropomorphic manipulators. The range of industrial applications for anthropomorphic manipulators is wide, given their versatility and dexterity [7].

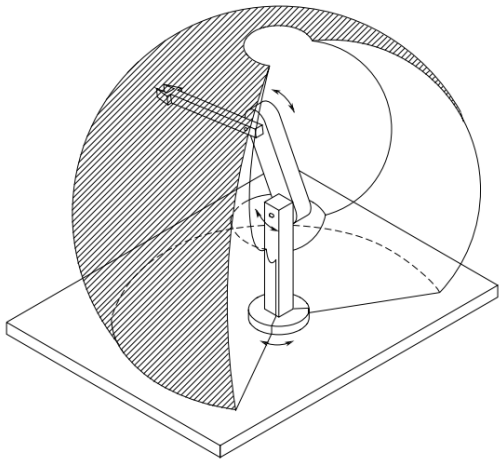

Figure I. 10: Anthropomorphic manipulator and its workspace [7].

Based on the latest report by the International Federation of Robotics (IFR), as of 2005, 59% of installed robot manipulators worldwide have anthropomorphic geometry, followed by 20% with Cartesian geometry, 12% with cylindrical geometry, and 8% with SCARA geometry [7].

I.5.3 Motion Characteristics:

A manipulator is defined as a planar manipulator if it has a "planar mechanism," which is useful for manipulating objects on a plane. On the other hand, if a manipulator has a "spherical mechanism," it is referred to as a spherical manipulator, which is useful as a pointing device. If the motion of a rigid body cannot be defined as planar or spherical, it is referred to as "spatial motion." If at least one moving link of a mechanism undergoes general spatial motion, the manipulator is defined as a "spatial manipulator"[8].

I.5.4 Drive technology:

While there are three primary drive technologies," electric, hydraulic, and pneumatic", most manipulators employ electric servo motors or stepper motors. This is due to the clear advantages of electric motors. However, it is worth noting that hydraulic and pneumatic drives offer some benefits, such as high-load carrying capabilities [8].

I.5.5 Kinematic structure:

Robots can also be categorized according to their kinematic structures. A robot with an open loop chain kinematic structure is called a "serial robot" or "open loop manipulator." On the other hand, a robot that has a closed loop-chain kinematic structure is known as a "parallel manipulator." In addition, a robot system that consists of both structure types is called a "hybrid manipulator"[8].

I.6 Types of Robot Joints:

The objective of a joint is to facilitate controlled relative movement between the input and output links. Most industrial robots have mechanical joints that can be grouped into one of five categories, comprising two types that deliver linear motion and three that provide rotary motion. Each joint has a specific range over which it can be maneuvered. The figures below depict the five joint types [8].

I.6.1 Linear joint

A linear sliding motion characterizes the movement between the input and output links, and the axes of the two links are parallel (**Figure I.11**).

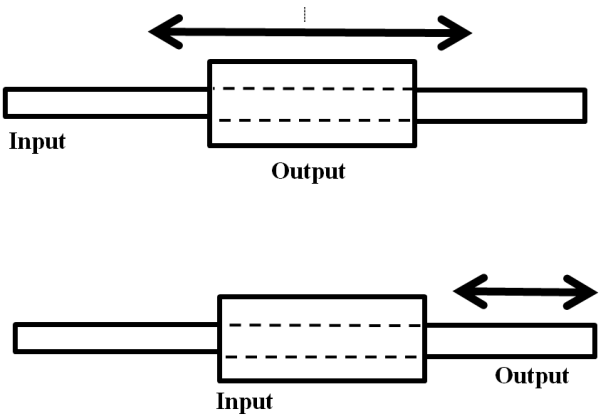

Figure I. 11: Linear joint.

I.6.2 Orthogonal joint

Similar to the previous joint type, this joint also facilitates linear sliding motion. However, in this case, the input and output links are perpendicular to each other during the motion.

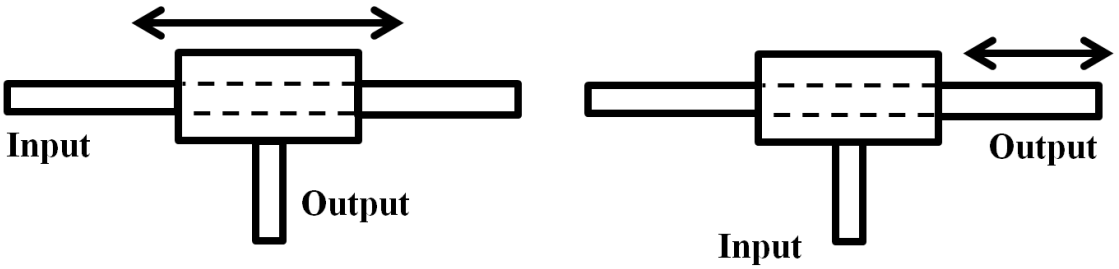

Figure I. 12: Linear joint.

I.6.3 Rotational joint

This joint type enables relative rotational motion of the joints, with the axis of rotation being perpendicular to the axes of the input and output links (as shown in Figure I.13).

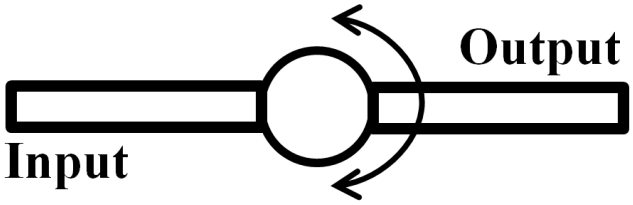

Figure I. 13: Rotational joint.

I.6.4 Twisting joint:

This joint type also entails a rotary motion, but the axis of rotation runs parallel to the axes of the two links (**Figure I.14**).

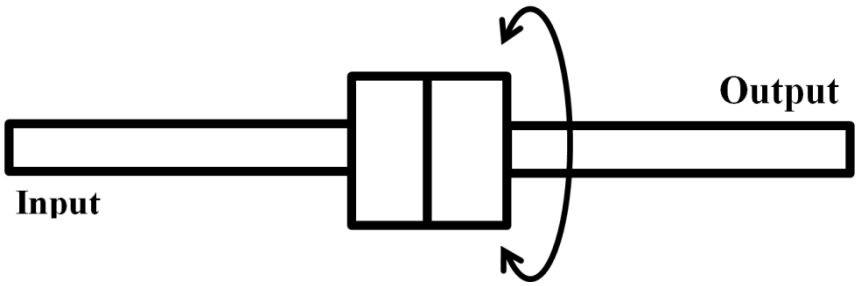

Figure I. 14: Twisting joint.

I.6.5 Revolving joint:

This type of joint features an input link axis that runs parallel to the joint's rotation axis, while the output link axis is oriented perpendicular to it (**Figure I.15**).

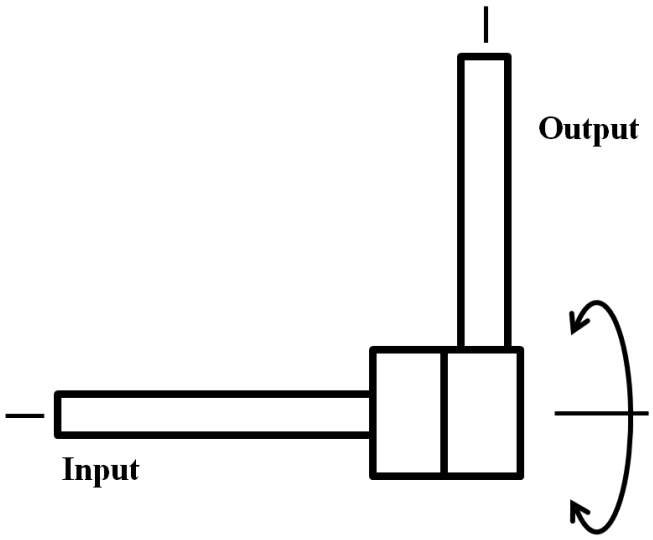

Figure I. 15: Revolving joint.

I.7 Robot Manipulators:

A robot manipulator's mechanical structure comprises a series of rigid bodies or links that are connected through articulations or joints. The manipulator is characterized by an arm that provides mobility, a wrist that imparts dexterity, and an end-effector that

accomplishes the robot's required task. There are three main types of robot manipulators: series, parallel, and hybrid manipulators [7].

I.7.1 Serial Manipulators:

Serial manipulators, which consist of a series of rigid links connected by joints, are the most commonly used industrial robots. Their joints are usually revolute.

Most serial manipulators have an anthropomorphic arm structure with a "shoulder" (first two joints), an "elbow" (third joint), and a "wrist" (last three joints). To position and orient an object in an arbitrary position and orientation in the robot's workspace, at least six degrees of freedom are required, which is why most serial robots have six joints.

Despite their advantages, such as a larger workspace and the ability to reach high speeds and accelerations, serial manipulators also have some drawbacks, such as accumulated and amplified errors, and a lack of energy efficiency.

In contrast to serial manipulators, SCARA robots, which are among the most common types, have only four degrees of freedom and are typically used in "pick and place" applications.[3]

Figure I. 16: Serial robot (Mitsubishi) [10].

I.7.2 Parallel Manipulators:

A parallel manipulator is a closed chain mechanism consisting of a fixed (base) and a movable (end effector) platform, which are connected by a number of "legs."

Each leg is connected to the platforms by spherical or universal joints and controlled by an actuator. The degree of freedom depends on the number of actuated legs. Parallel manipulators are known for their accurate position capabilities and light constructions, as the links only feel traction or compression forces, not bending. Furthermore, actuators can be placed in the base platform, reducing the weight of the movable construction (Bruyninckx et al, 2001).

One of the main advantages of parallel manipulators is their high structural stiffness and load capacity, which make them suitable for high-precision tasks. They also have high bandwidth motion capability, allowing for fast and precise movements.

However, parallel manipulators have some disadvantages, such as a limited workspace and a loss of stiffness in singular positions, which can cause stability issues [8].

Figure I. 17: Parallel Manipulators [11].

I.7.3 Hybrid Manipulators:

Parallel manipulators are the preferred choice for robots that require features such as precision, high speed, and rigidity. However, due to the limited workspace of parallel manipulators, open-kinematic serial manipulators are more commonly used in industrial robots for a wide range of applications. To address this limitation, hybrid

manipulators that combine the advantages of both parallel and serial manipulators have been developed. These manipulators typically consist of one manipulator in series and one in parallel or two manipulators in parallel, and can overcome the workspace limitations of parallel manipulators. Hybrid manipulators offer increased degrees of freedom and are composed of two different parallel manipulators in their kinematic chain [3].

I.8 Motion Control of Robot Manipulators:

I.8.1 point-to-point:

The "point-to-point" method is the easiest way to define the movement of a manipulator. This approach involves identifying a sequence of points within the manipulator's workspace that the end-effector must traverse (**Figure I.18**). Therefore, the objective of position control is to guide the end-effector towards a specific point, regardless of the trajectory it follows from its initial state [10].

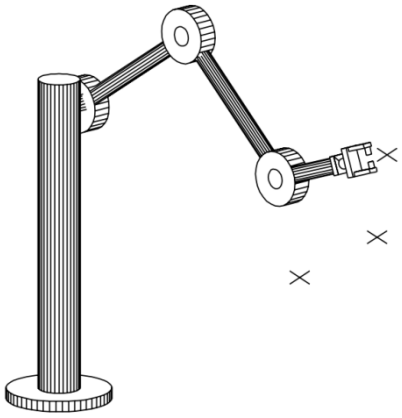

Figure I. 18: Point-to-point motion specification [12].

I.8.2 Through a continuous trajectory:

An alternative method for defining a robot's motion is through a continuous trajectory, a continuous curve or path in the state space, parameterized in time, to accomplish a task. This method's motion control problem is making the end-effector follow the trajectory as closely as possible (**Figure I.19**). This control problem, which is the central objective of our study, is also known as trajectory tracking control.

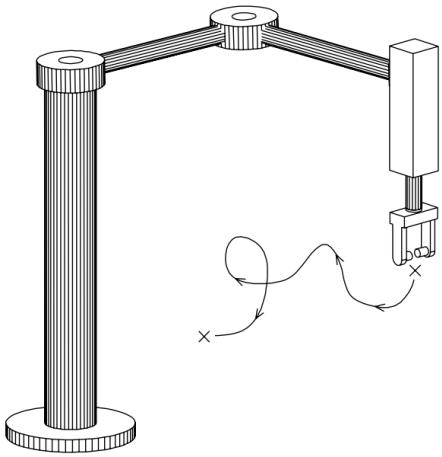

Figure I. 19: Trajectory motion specification [12].

I.8.3 Path planning

Path planning is the process of determining a state space curve that connects the end-effector's desired initial and final posture while avoiding any obstacles. Trajectory generation involves parameterizing the curve obtained during path planning over time. The resulting time-parameterized trajectory, commonly referred to as the reference trajectory, is primarily obtained regarding workspace coordinates. Using the inverse kinematics method, a time-parameterized trajectory for the joint coordinates can be obtained. The control design process aims to solve the control problem mentioned above.

I.9 Conclusion

In this chapter we presented the essential notions of robotics, starting by defining robotics and presented the different types and characteristics of robots, then we demonstrated the types of joints, finally we have gave overview on the steps of motion control of robots.

CHAPITRE II:

MATHEMATICAL MODELING

II.1 introduction

Mathematical models are essential for controlling a robot or simulating its behavior. These models are designed based on specific objectives, task constraints, and desired performance. Generally, there are three types of models that can be employed: geometric models, kinematic models, and dynamic models [3].

The level of difficulty involved in creating mathematical models for robot kinematics depends on the complexity of the mechanical structure and its degrees of freedom. Mathematical concepts and tools are utilized to describe the movement and other characteristics of manipulators. Additionally, these tools are used to develop and assess algorithms that enable robots to perform specific movements and execute desired tasks. Computer programming is also used to facilitate the computation involved in these operations [12].

This chapter will provide an overview of the mathematical formalism associated with each type of modeling. Specifically, it will cover the geometric, kinematic and dynamic models.

II.2. Homogeneous coordinates

II.2.1. Representation of a point:

Let $\left({}^{i}P_x,\ {}^{i}P_y,\ {}^{i}P_z\right)$ denote the Cartesian coordinates of an arbitrary point **P** with respect to the frame $\mathbf{R_i}$, which is characterized by the origin $\mathbf{O_i}$ and the axes $\mathbf{x_i}, \mathbf{y_i}, \mathbf{z_i}$ **(Figure II.1)**. The homogeneous coordinates of point **P** relative to frame $\mathbf{R_i}$ are given by $({}^{i}P_x, w{}^{i}P_y, w{}^{i}P_z, w)$, where **w** represents a scaling factor. In robotics, the value of **w** is usually set to **1**, and the homogeneous coordinates of point **P** are therefore represented by a column vector of size (4×1).

$$ {}^{i}\mathbf{P} = \begin{bmatrix} {}^{i}P_x \\ {}^{i}P_y \\ {}^{i}P_z \\ 1 \end{bmatrix} \qquad [2.1] $$

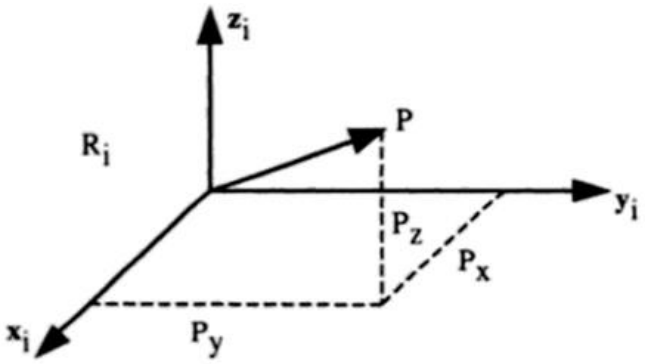

Figure II.1: Representation of a point vector [14].

II.2.2. Representation of a direction:

A direction, which is a free vector, is also represented by four components, but the fourth component is typically set to zero to indicate a vector at infinity. If the Cartesian coordinates of a unit vector **u** with respect to frame $\mathbf{R_i}$ are given by $({}^{i}u_x, {}^{i}u_y, {}^{i}u_z)$, its homogeneous coordinates can be expressed as:

$$ {}^{i}\mathbf{u} = \begin{bmatrix} {}^{i}u_x \\ {}^{i}u_y \\ {}^{i}u_z \\ 0 \end{bmatrix} \qquad [2.2] $$

II.3. Homogeneous transformations

II.3.1. Transformation of frames:

The transformation, translation and/or rotation, of a frame $\mathbf{R_i}$ into frame $\mathbf{R_j}$ **(Figure II.2)** is represented by the (4x4) homogeneous transformation matrix $^{\mathbf{i}}\mathbf{T_j}$ such that:

$$^{i}\mathbf{T_j} = \left[{}^{i}\mathbf{s_j} \;\; {}^{i}\mathbf{n_j} \;\; {}^{i}\mathbf{a_j} \;\; {}^{i}\mathbf{P_j} \right] = \begin{bmatrix} \mathbf{s_x} & \mathbf{n_x} & \mathbf{a_x} & \mathbf{P_x} \\ \mathbf{s_y} & \mathbf{n_y} & \mathbf{a_y} & \mathbf{P_y} \\ \mathbf{s_z} & \mathbf{n_z} & \mathbf{a_z} & \mathbf{P_z} \\ \mathbf{0} & \mathbf{0} & \mathbf{0} & \mathbf{1} \end{bmatrix} = \begin{bmatrix} {}^{i}\mathbf{s_j} & {}^{i}\mathbf{n_j} & {}^{i}\mathbf{a_j} & {}^{i}\mathbf{P_j} \\ \mathbf{0} & \mathbf{0} & \mathbf{0} & \mathbf{1} \end{bmatrix} \qquad [2.3]$$

The components of the unit vectors along the $\mathbf{x_j}, \mathbf{y_j}$ and $\mathbf{z_j}$ axes in frame $\mathbf{R_i}$ are contained in $^{\mathbf{i}}\mathbf{s_j}$, $^{\mathbf{i}}\mathbf{n_j}$ and $^{\mathbf{i}}\mathbf{a_j}$ respectively, while the vector representing the coordinates of the origin of frame $\mathbf{R_j}$ expressed in frame $\mathbf{R_i}$ is denoted by $^{\mathbf{i}}\mathbf{P_j}$.

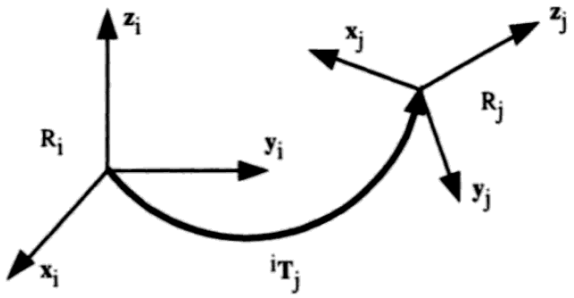

Figure II.2: Transformation of frames [14].

II.3.2. Transformation matrix of a pure translation:

The transformation denoted by **Trans(a, b, c)** represents a translation along the x, y, and z axes, where a, b, and c are the respective translation distances. As the orientation remains unchanged, the transformation can be expressed as **(Figure II.3)**:

$$^{i}\mathbf{T_j} = \mathbf{Trans(a, b, c)} = \begin{bmatrix} \mathbf{1} & \mathbf{0} & \mathbf{0} & \mathbf{a} \\ \mathbf{0} & \mathbf{1} & \mathbf{0} & \mathbf{b} \\ \mathbf{0} & \mathbf{0} & \mathbf{1} & \mathbf{c} \\ \mathbf{0} & \mathbf{0} & \mathbf{0} & \mathbf{1} \end{bmatrix} \quad [2.4]$$

Moving forward, we will adopt the notation **Trans(u, d)** to represent a translation along an axis **u** by **a** distance of **d**. Consequently, the matrix **Trans(a, b, c)** can be expressed as the product of three matrices: **Trans(x, a)**, **Trans(y, b)**, and **Trans(z, c)**, which can be multiplied in any order.

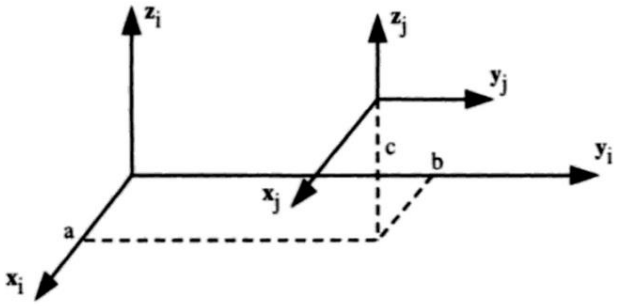

Figure II.3: Transformation of pure translation [14].

II.3.3 Transformation matrices of a rotation about the principle axes:

Let **Rot(x, θ)** be this transformation matrices of a rotation about the x-axis by an angle **θ**. From **(Figure II.4)**.

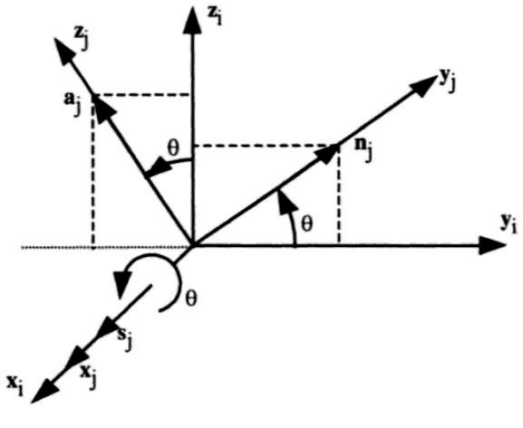

Figure II.4: Transformation of a pure rotation about the x-axis [14].

We can infer that the components of the unit vectors ${}^{i}\mathbf{s_j}$, ${}^{i}\mathbf{n_j}$ and ${}^{i}\mathbf{a_j}$ along the $\mathbf{x_j}$, $\mathbf{y_j}$, and $\mathbf{z_j}$ axes of frame $\mathbf{R_j}$, respectively, expressed in frame $\mathbf{R_i}$ are given by the following expressions:

$$\begin{cases} {}^{i}\mathbf{s_j} = [\mathbf{1} \quad \mathbf{0} \quad \mathbf{0} \quad \mathbf{0}]^{\mathbf{T}} \\ {}^{i}\mathbf{n_j} = [\mathbf{0} \quad \mathbf{C\theta} \quad \mathbf{S\theta} \quad \mathbf{0}]^{\mathbf{T}} \\ {}^{i}\mathbf{a_j} = [\mathbf{0} \quad -\mathbf{S\theta} \quad \mathbf{C\theta} \quad \mathbf{0}]^{\mathbf{T}} \end{cases} \qquad [2.5]$$

Where $\mathbf{S\theta}$ and $\mathbf{C\theta}$ represent $\mathbf{\sin(\theta)}$ and $\mathbf{\cos(\theta)}$ respectively, and the superscript $\mathbf{T}$ indicates the transpose of the vector.

$$ {}^{i}\mathbf{T_j} = \mathbf{Rot(x,\theta)} = \begin{bmatrix} \mathbf{1} & \mathbf{0} & \mathbf{0} & \mathbf{0} \\ \mathbf{0} & \mathbf{C\theta} & -\mathbf{S\theta} & \mathbf{0} \\ \mathbf{0} & \mathbf{S\theta} & \mathbf{C\theta} & \mathbf{0} \\ \mathbf{0} & \mathbf{0} & \mathbf{0} & \mathbf{1} \end{bmatrix} = \begin{bmatrix} & & & \mathbf{0} \\ & \mathbf{Rot(x,\theta)} & & \mathbf{0} \\ & & & \mathbf{0} \\ \mathbf{0} & \mathbf{0} & \mathbf{0} & \mathbf{1} \end{bmatrix} \qquad [2.6]$$

In the same way, we obtain the transformation matrices of a rotation about the y-axis by an angle $\mathbf{\theta}$.

$$ {}^{i}\mathbf{T_j} = \mathbf{Rot(y,\theta)} = \begin{bmatrix} \mathbf{C\theta} & \mathbf{0} & \mathbf{S\theta} & \mathbf{0} \\ \mathbf{0} & \mathbf{1} & \mathbf{0} & \mathbf{0} \\ -\mathbf{S\theta} & \mathbf{0} & \mathbf{C\theta} & \mathbf{0} \\ \mathbf{0} & \mathbf{0} & \mathbf{0} & \mathbf{1} \end{bmatrix} = \begin{bmatrix} & & & \mathbf{0} \\ & \mathbf{Rot(y,\theta)} & & \mathbf{0} \\ & & & \mathbf{0} \\ \mathbf{0} & \mathbf{0} & \mathbf{0} & \mathbf{1} \end{bmatrix} \qquad [2.7]$$

We can also verify the transformation matrices of a rotation about the z-axis by an angle $\mathbf{\theta}$.

$$ {}^{i}\mathbf{T_j} = \mathbf{Rot(z,\theta)} = \begin{bmatrix} \mathbf{C\theta} & -\mathbf{S\theta} & \mathbf{0} & \mathbf{0} \\ \mathbf{S\theta} & \mathbf{C\theta} & \mathbf{0} & \mathbf{0} \\ \mathbf{0} & \mathbf{0} & \mathbf{1} & \mathbf{0} \\ \mathbf{0} & \mathbf{0} & \mathbf{0} & \mathbf{1} \end{bmatrix} = \begin{bmatrix} & & & \mathbf{0} \\ & \mathbf{Rot(z,\theta)} & & \mathbf{0} \\ & & & \mathbf{0} \\ \mathbf{0} & \mathbf{0} & \mathbf{0} & \mathbf{1} \end{bmatrix} \qquad [2.8]$$

II.3.4. Properties of homogeneous transformation matrices:

From equation [2.3], a transformation matrix can be written as:

$$ \mathbf{T} = \begin{bmatrix} \mathbf{s_x} & \mathbf{n_x} & \mathbf{a_x} & \mathbf{P_x} \\ \mathbf{s_y} & \mathbf{n_y} & \mathbf{a_y} & \mathbf{P_y} \\ \mathbf{s_z} & \mathbf{n_z} & \mathbf{a_z} & \mathbf{P_z} \\ \mathbf{0} & \mathbf{0} & \mathbf{0} & \mathbf{1} \end{bmatrix} = \begin{bmatrix} & \mathbf{A} & & \mathbf{P} \\ \mathbf{0} & \mathbf{0} & \mathbf{0} & \mathbf{1} \end{bmatrix} \qquad [2.9]$$

The matrix **A** represents the rotation whereas the column matrix **P** represents the translation.

If a frame $\mathbf{R_0}$ is subjected to **k** consecutive transformations **(Figure II.5)** and if each transformation **i, (i=1,.. k)**, is defined with respect to the current frame $\mathbf{R_{i-1}}$, then the transformation $^{0}\mathbf{R_k}$ can be deduced by multiplying all the transformation on the right as:

$$^{0}\mathbf{T_k} = {}^{0}\mathbf{T_1}\ {}^{1}\mathbf{T_2}\ {}^{2}\mathbf{T_3} \dots {}^{k-1}\mathbf{T_k} \qquad [2.10]$$

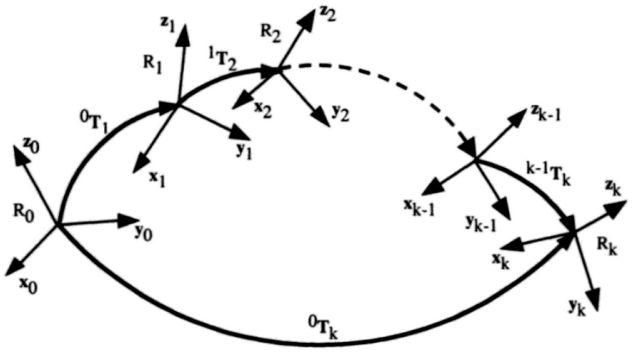

Figure II.5: Composition of transformation: multiplication on the right [14].

II.4. model of serial robots:

To design and control a robot, it is necessary to calculate various mathematical models, including transformation models between the joint space and the task space. These models can be classified into two categories: direct and inverse geometric models, direct and inverse kinematic models, and dynamic models [14].

II.4.1 geometric models:

Geometric models are mathematical models that provide the position of the end-effector in relation to the joint variables of the mechanism, and vice versa.

II.4.1.1. Description of the geometry of serial robot:

A serial robot consists of **n+1** links and **n** joints, where the links are rigid and the joints are ideal and can be either revolute or prismatic. To represent a complex joint, it

can be converted into an equivalent combination of revolute and prismatic joints with zero-length massless links. The links are numbered in a sequence from link **0** at the base to link **n** at the terminal end (**Figure II.6**).

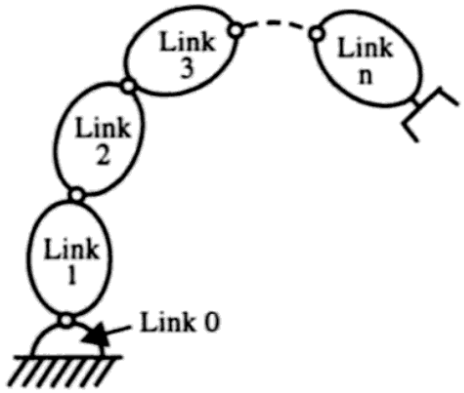

Figure II.6: Robot with simple open structure [14].

With reference to **(Figure II.17)**, let Axis **i** denote the axis of the joint connecting Link $\mathbf{i-1}$ to Link **i**; the so-called Denavit-Hartenberg convention is adopted to define link Frame **i** [7]:

- Choose axis $\mathbf{Z_i}$ along the axis of Joint $\mathbf{i+1}$.
- Locate the origin $\mathbf{O_i}$ at the intersection of axis $\mathbf{Z_i}$ with the common normal to axes $\mathbf{Z_{i-1}}$ and $\mathbf{Z_i}$.
- Choose axis along the common normal to axes $\mathbf{Z_{i-1}}$ and $\mathbf{Z_i}$ with direction from Joint **i** to Joint $\mathbf{i+1}$.
- Choose axis $\mathbf{Y_i}$ so as to complete a right-handed frame.

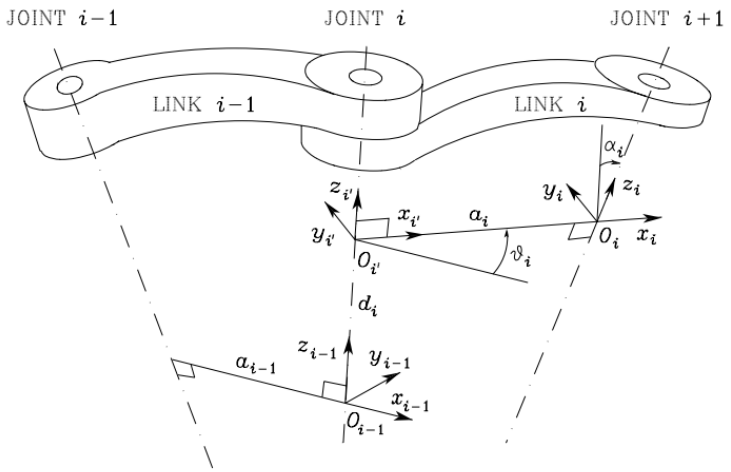

Figure II.7: Denavit-Hartenberg kinematic parameters [7].

Once the link frames have been established, the position and orientation of Frame **i** with respect to Frame $\mathbf{i-1}$ are completely specified by the following parameters [7]:

$\mathbf{a_i}$ = the distance from $\mathbf{Z_{i-1}}$ to $\mathbf{Z_i}$ measured along $\mathbf{X_i}$.

$\boldsymbol{\alpha_i}$ = the angle from $\mathbf{Z_{i-1}}$ to $\mathbf{Z_i}$ measured about $\mathbf{X_i}$.

$\mathbf{d_i}$ = the distance from $\mathbf{X_{i-1}}$ to $\mathbf{X_i}$ measured along $\mathbf{Z_{i-1}}$.

$\boldsymbol{\theta_i}$= the angle from $\mathbf{X_{i-1}}$ to $\mathbf{X_i}$ measured about $\mathbf{Z_{i-1}}$.

The transformation matrix defining frame $\mathbf{R_i}$ relative to frame $\mathbf{R_{i-1}}$ is given as (**Figure II.7**).

$$^{\mathbf{i-1}}\mathbf{T_i} = \mathbf{Rot}(\mathbf{z_{i-1}}, \boldsymbol{\theta_i}) \cdot \mathbf{Trans}(\mathbf{z_{i-1}}, \mathbf{d_i}) \cdot \mathbf{Rot}(\mathbf{x}, \boldsymbol{\alpha_i}) \cdot \mathbf{Trans}(\mathbf{x}, \mathbf{a_i}) \quad [2.11]$$

$$^{\mathbf{i-1}}\mathbf{T_i} = \begin{bmatrix} \mathbf{C\theta_i} & \mathbf{-S\theta_i C\alpha_i} & \mathbf{S\theta_i S\alpha_i} & \mathbf{a_i C\theta_i} \\ \mathbf{S\theta_i} & \mathbf{C\theta_i C\alpha_i} & \mathbf{-C\theta_i S\alpha_i} & \mathbf{a_i S\theta_i} \\ \mathbf{0} & \mathbf{S\alpha_i} & \mathbf{C\alpha_i} & \mathbf{d_i} \\ \mathbf{0} & \mathbf{0} & \mathbf{0} & \mathbf{1} \end{bmatrix} \quad [2.12]$$

II.4.1.2 Direct geometric model:

The Direct Geometric Model (DGM) defines the position of a robot's end-effector in terms of its joint coordinates. In a serial robot structure, this relationship can be expressed as a transformation matrix $^{\mathbf{0}}\mathbf{T_n}$, where **n** represents the terminal link [12]:

$$^{0}\mathbf{T}_{n} = {}^{0}\mathbf{T}_{1}(\mathbf{q}_{1})\,{}^{1}\mathbf{T}_{2}(\mathbf{q}_{2}) \ldots {}^{n-1}\mathbf{T}_{n}(\mathbf{q}_{n}) \quad [2.13]$$

The direct geometric model of a robot may also be represented by the relation:

$$\mathbf{X} = \mathbf{f}(\mathbf{q}) \quad [2.14]$$

Where **q** is the vector of joint variables such that:

$$\mathbf{q} = [\mathbf{q}^{1}\ \mathbf{q}^{2} \ldots\ \mathbf{q}^{n}]^{T} \quad [2.15]$$

The position and orientation of the terminal link are defined as:

$$\mathbf{X} = [\mathbf{x}^{1}\ \mathbf{x}^{1} \ldots\ \mathbf{x}^{1}]^{T} \quad [2.16]$$

There are several possibilities of defining the vector **X**. For example, with the elements of the matrix $^{0}\mathbf{T}_{n}$:

$$\mathbf{X} = [\mathbf{P}_{x}\ \ \mathbf{P}_{y}\ \ \mathbf{P}_{z}\ \ \mathbf{s}_{x}\ \ \mathbf{s}_{y}\ \ \mathbf{s}_{z}\ \ \mathbf{n}_{x}\ \ \mathbf{n}_{y}\ \ \mathbf{n}_{z}\ \ \mathbf{a}_{x}\ \ \mathbf{a}_{y}\ \ \mathbf{a}_{z}]^{T} \quad [2.17]$$

Taking into account that $\mathbf{s} = \mathbf{n} \times \mathbf{a}$, we can also take:

$$\mathbf{X} = [\mathbf{P}_{x}\ \ \mathbf{P}_{y}\ \ \mathbf{P}_{z}\ \ \mathbf{n}_{x}\ \ \mathbf{n}_{y}\ \ \mathbf{n}_{z}\ \ \mathbf{a}_{x}\ \ \mathbf{a}_{y}\ \ \mathbf{a}_{z}]^{T} \quad [2.18]$$

II.4.1.3 Inverse geometric model:

The inverse geometric model enables the determination of the joint variable vector from the operational coordinate vector. This model can be expressed as follows [3]:

$$\mathbf{q} = \mathbf{f}^{-1}(\mathbf{x}) \quad [2.19]$$

Among the methods used to determine the inverse geometric model are:

- Geometric methods: They make it possible to determine the vector **q** by using geometric transformations by taking advantage of the particular structure of the manipulator considered.
- Algebraic methods: They make it possible to determine the vector **q** by performing algebraic transformations on equation [2.18]. Among the methods used, we cite the method of Paul.

Let $\mathbf{U_0}$ be the desired situation for the end device, such that:

$$\mathbf{U_0} = \begin{bmatrix} \mathbf{s_x} & \mathbf{n_x} & \mathbf{a_x} & \mathbf{P_x} \\ \mathbf{s_y} & \mathbf{n_y} & \mathbf{a_y} & \mathbf{P_y} \\ \mathbf{s_z} & \mathbf{n_z} & \mathbf{a_z} & \mathbf{P_z} \\ \mathbf{0} & \mathbf{0} & \mathbf{0} & \mathbf{1} \end{bmatrix} \quad [2.20]$$

PAUL's method consists in solving a system of equations obtained by pre-multiplying successively the two sides of equation [2.21] by the inverse homogeneous matrices $^{\mathbf{i}}\mathbf{T_{i-1}}$ with (i=1…n-1).

$$\mathbf{U_0} = {}^{\mathbf{0}}\mathbf{T_n} \quad [2.21]$$

In the process of solving the inverse geometric problem, the following situations can arise:

- The problem may have a finite number of solutions that can be calculated unambiguously.
- It may be impossible to find a solution when the desired position cannot be reached by the robot.
- In cases where the robot has redundant degrees of freedom or passes through a singular configuration, there may be several possible solutions

II.4.2 kinematic model:

The direct and inverse kinematic models provide a relationship between the velocity of the end-effector and the joint velocities, as well as vice versa.

II.4.2.1 Direct kinematic model:

The direct kinematic model expresses the end-effector's velocity ($\dot{X}$) in relation to the joint velocities ($\dot{q}$) of the robot manipulator. The mathematical expression for this relationship is typically written as:

$$\dot{\mathbf{X}} = \mathbf{J}(\mathbf{q})\dot{\mathbf{q}} \quad [2.22]$$

where $\mathbf{J}(\mathbf{q})$ denotes the $(\mathbf{m} \times \mathbf{n})$ Jacobian matrix, where m is the number of degrees of freedom of the manipulator robot and n is the number of joints

The Jacobian matrix can be obtained by differentiating the DGM, $\mathbf{X} = \mathbf{f}(\mathbf{q})$ using the partial derivative $\frac{\partial \mathbf{f}}{\partial \mathbf{q}}$ such that:

$$\mathbf{J_{ij}} = \frac{\partial \mathbf{f_i(q)}}{\partial \mathbf{q_j}}; \quad \text{For} \quad \mathbf{i = 1 \ldots m} \quad \text{and} \quad \mathbf{j = 1 \ldots n} \qquad [2.23]$$

Where $\mathbf{J_{ij}}$ is the $(\mathbf{i}, \mathbf{j})$ element of the Jacobian matrix $\mathbf{J}$.

II.4.2.2 Inverse kinematic model:

The inverse kinematic model determines the joint angles necessary to achieve a desired end-effector position and orientation. The inverse kinematic model typically involves solving equations that relate the end-effector position and orientation to the joint angles. There are many approaches to solving the inverse kinematics problem, including analytical, geometric, and numerical methods. The inverse kinematic model gives the joint velocities $\dot{\mathbf{q}}$ for a desired end effector velocity $\dot{\mathbf{X}}$. In this case, the Jacobian matrix $\mathbf{J}$ is square and of total rank. Thus, moving the end-effector with finite velocity in any desired direction of the task space is possible. We compute $\mathbf{J^{-1}}$, the inverse of $\mathbf{J}$, either numerically or analytically. Then, the joint velocity vector $\dot{\mathbf{q}}$ is obtained as [6][12][13]:

$$\dot{\mathbf{q}} = \mathbf{J^{-1}}\,\dot{\mathbf{X}} \qquad [2.24]$$

The equation [2.20] solution exists if J has full rank; this is valid if the manipulator does not pass through a particular configuration.

For redundant manipulators, the inverse kinematic model admits several possible solutions. Optimizing an objective function guides the choice of a solution among several [3].

II.4.3 Dynamic model:

Dynamic models give the relations between the input torques or forces of the actuators and the positions, velocities and accelerations of the joints [14]. The formalisms most used for calculating the inverse dynamic model are the Formalism of Lagrange and the Formalism of Newton-Euler [3].

Dynamic models give the relations between the input torques or forces of the actuators and the positions, velocities and accelerations of the joints. The formalisms most used for calculating the inverse dynamic model are the Formalism of Lagrange and the Formalism of Newton-Euler. The Newton-Euler equations of motion can be used to derive the dynamic model of a robot, known as the dynamic equation and describe the relationship between forces and moments acting on the robot. The dynamic equation can be expressed in the following form:

$$\mathbf{M}(\mathbf{q})\ddot{\mathbf{q}} + \mathbf{C}(\mathbf{q},\dot{\mathbf{q}})\dot{\mathbf{q}} + \mathbf{g}(\mathbf{q}) = \boldsymbol{\tau} \qquad [2.25]$$

Where $\mathbf{M}(\mathbf{q})$ is the mass matrix, $\mathbf{q}$ is the joint position vector, $\dot{\mathbf{q}}$ is the joint velocity vector, $\ddot{\mathbf{q}}$ is the joint acceleration vector, $\mathbf{C}(\mathbf{q},\dot{\mathbf{q}})$ is the Coriolis and centrifugal forces matrix, $\mathbf{g}(\mathbf{q})$ is the gravity forces vector, and $\boldsymbol{\tau}$ is the joint torque vector.

The Newton-Euler formalism is especially useful for robotic systems with a tree-like structure, such as serial and parallel robots. It uses the principles of Newton's laws and Euler's equations to derive the equations of motion of the robot. The Lagrange formalism, on the other hand, is more general and can be applied to a broader range of mechanical systems, including robots with closed kinematic chains [7][16][17].

II.5 Conclusion

In this chapter of mathematical modeling, we have described the geometric modeling of manipulator robots, its great interest in robotics, as well as the calculation by the Denavit-Hartenberg method, and the obtaining of the inverse geometric model.

We then defined kinematic modeling, as well as obtaining it using the DGM derivation method, which was used to develop the inverse kinematic model. These models allow us to develop a kinematic control law to control the speed of our robot.

CHAPITRE III:
STUDY OF THE SCARA ROBOT RRPR MODELS

III.1 Introduction

In this chapter, we will study the different geometric, and kinematic modeling of the RRPR-type SCARA robot. It consists of three revolute joints and one prismatic joint.

First, we will determine the homogeneous transition matrix using the DH parameters and then the coordinates of end-effector position. And also we will use the Inverse geometric model to determine the equations of angle position.

Finally, operational velocity and joint velocity will be determined using the kinematic model.

III.2 Direct geometric model of the SCARA robot

Our SCARA robot is RRPR with four degrees of the freedom. Let's consider a robot with three revolute joints ($\boldsymbol{\theta_1}$,$\boldsymbol{\theta_2}$,$\boldsymbol{\theta_4}$) and one prismatic joint ($\mathbf{d_3}$), with the base at the origin of the coordinate system. The landmarks are established in (**FigureIII.1**) based on the Denavit-Hartenberg (DH) principle.

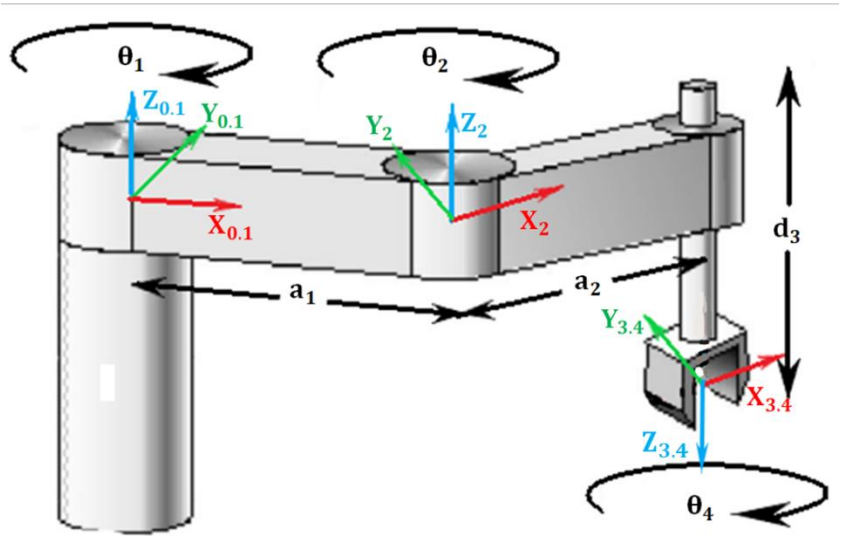

Figure III.1: Scheme of a SCARA RRPR-Type

Based on the robot diagram, we can create the DH parameters in the following table:

Table III.1 : Denavit-Hartenberg parameter assignment.

i	a_i	α_i	d_i	θ_i
1	a_1	0°	0	θ_1
2	a_2	180°	0	θ_2
3	0	0°	d_3	0°
4	0	0°	0	θ_4

III.2.1 Calculation of transformation matrix

We will now insert the parameters in the general formula of the transformation matrix $^{i-1}\mathbf{T_i}$ that we saw in chapter II:

$$^{i-1}\mathbf{T_i} = \begin{bmatrix} \mathbf{C\theta_i} & \mathbf{-S\theta_i C\alpha_i} & \mathbf{S\theta_i S\alpha_i} & \mathbf{a_i C\theta_i} \\ \mathbf{S\theta_i} & \mathbf{C\theta_i C\alpha_i} & \mathbf{-C\theta_i S\alpha_i} & \mathbf{a_i S\theta_i} \\ \mathbf{0} & \mathbf{S\alpha_i} & \mathbf{C\alpha_i} & \mathbf{d_i} \\ \mathbf{0} & \mathbf{0} & \mathbf{0} & \mathbf{1} \end{bmatrix} \quad [2.12]$$

The **Cos**( ) and **sin**( ) are replaced by **C** and **S** respectively to simplify the equation.

From **Table (III.1)** and the use of equation [2.12], we deduce the following geometric relations:

$$^{0}\mathbf{T_1} = \begin{bmatrix} \mathbf{C\theta_1} & \mathbf{-S\theta_1} & \mathbf{0} & \mathbf{0} \\ \mathbf{S\theta_1} & \mathbf{C\theta_1} & \mathbf{0} & \mathbf{0} \\ \mathbf{0} & \mathbf{0} & \mathbf{1} & \mathbf{0} \\ \mathbf{0} & \mathbf{0} & \mathbf{0} & \mathbf{1} \end{bmatrix} \quad [3.1]$$

$$^{1}\mathbf{T_2} = \begin{bmatrix} \mathbf{C\theta_2} & \mathbf{-S\theta_2} & \mathbf{0} & \mathbf{a_1} \\ \mathbf{S\theta_2} & \mathbf{C\theta_2} & \mathbf{0} & \mathbf{0} \\ \mathbf{0} & \mathbf{0} & \mathbf{1} & \mathbf{0} \\ \mathbf{0} & \mathbf{0} & \mathbf{0} & \mathbf{1} \end{bmatrix} \quad [3.2]$$

$$^{2}\mathbf{T_3} = \begin{bmatrix} \mathbf{1} & \mathbf{0} & \mathbf{0} & \mathbf{a_2} \\ \mathbf{0} & \mathbf{-1} & \mathbf{0} & \mathbf{0} \\ \mathbf{0} & \mathbf{0} & \mathbf{-1} & \mathbf{d_3} \\ \mathbf{0} & \mathbf{0} & \mathbf{0} & \mathbf{1} \end{bmatrix} \quad [3.3]$$

$$^{3}\mathbf{T_4} = \begin{bmatrix} \boldsymbol{C\theta_4} & \boldsymbol{-S\theta_4} & \mathbf{0} & \mathbf{0} \\ \boldsymbol{S\theta_4} & \boldsymbol{C\theta_4} & \mathbf{0} & \mathbf{0} \\ \mathbf{0} & \mathbf{0} & \mathbf{1} & \mathbf{0} \\ \mathbf{0} & \mathbf{0} & \mathbf{0} & \mathbf{1} \end{bmatrix} \quad [3.5]$$

We will calculate ${}^0T_4$:

$$\mathbf{{}^0T_4 = {}^0T_1\ {}^1T_2\ {}^2T_3\ {}^3T_4}$$

$$\mathbf{{}^0T_4} = \begin{bmatrix} \boldsymbol{C(\theta_1+\theta_2+\theta_4)} & \mathbf{-S(\theta_1+\theta_2+\theta_4)} & \mathbf{0} & \boldsymbol{a_1C\theta_1 + a_2C(\theta_1+\theta_2)} \\ \boldsymbol{S(\theta_1+\theta_2+\theta_4)} & \mathbf{C(\theta_1+\theta_2+\theta_4)} & \mathbf{0} & \boldsymbol{a_1S\theta_1 + a_2S(\theta_1+\theta_2)} \\ \mathbf{0} & \mathbf{0} & \mathbf{1} & \mathbf{-d_3} \\ \mathbf{0} & \mathbf{0} & \mathbf{0} & \mathbf{1} \end{bmatrix} \quad [3.5]$$

Where

$$\cos(\theta_1+\theta_2) = \cos(\theta_1)\times\cos(\theta_2) - \sin(\theta_1)\times\sin(\theta_2)$$

And

$$\sin(\theta_1+\theta_2) = \sin(\theta_1)\times\cos(\theta_2) + \cos(\theta_1)\times\sin(\theta_2)$$

And from chapter II we know that:

$$\mathbf{T} = \begin{bmatrix} \mathbf{s_x} & \mathbf{n_x} & \mathbf{a_x} & \mathbf{P_x} \\ \mathbf{s_y} & \mathbf{n_y} & \mathbf{a_y} & \mathbf{P_y} \\ \mathbf{s_z} & \mathbf{n_z} & \mathbf{a_z} & \mathbf{P_z} \\ \mathbf{0} & \mathbf{0} & \mathbf{0} & \mathbf{1} \end{bmatrix} \quad [2.9]$$

The end-effector position can be given by the following coordinates:

$$\begin{cases} \mathbf{P_x = a_1C\theta_1 + a_2C(\theta_1+\theta_2)} \\ \mathbf{P_y = a_1S\theta_1 + a_2S(\theta_1+\theta_2)} \\ \mathbf{P_z = -d_3} \end{cases} \quad [3.6]$$

III.3 Invers geometric model of the SCARA robot

Rearranging above [3.6] equations.

Solve for θ_2:

$$P_x{}^2 + P_y{}^2 = [a_1C\theta_1 + a_2C(\theta_1+\theta_2)]^2 + [a_1S\theta_1 + a_2S(\theta_1+\theta_2)]^2$$

$$P_x{}^2 + P_y{}^2 = a_1{}^2 + a_2{}^2 + 2a_1a_2C(\theta_1 + \theta_2)$$

$$C\theta_2 = \frac{P_x{}^2+P_y{}^2-(a_1{}^2+a_2{}^2)}{2a_1a_2} \qquad [3.7]$$

$$\theta_2 = \text{Atan2}\left[\frac{P_x{}^2+P_y{}^2-(a_1{}^2+a_2{}^2)}{2a_1a_2}\right] \qquad [3.8]$$

Solve for θ_1:

$$P_x = (a_1 + a_2C\theta_2)C\theta_1 - a_2S\theta_2C\theta_1$$

$$P_y = (a_1 + a_2C\theta_2)S\theta_1 - a_2S\theta_2S\theta_1$$

Let's take as

$$A = (a_1 + a_2C\theta_2) \text{ And } B = a_2S\theta_2$$

Rearranging above equation

$$P_x = AC\theta_1 - BC\theta_1$$

$$P_y = AS\theta_1 - BS\theta_1$$

$$\frac{P_x}{\sqrt{A^2+B^2}} = \frac{A}{\sqrt{A^2+B^2}}C\theta_1 - \frac{B}{\sqrt{A^2+B^2}}S\theta_1 \qquad [3.8]$$

$$\frac{P_x}{\sqrt{A^2+B^2}} = C(\gamma + \theta_1) \text{ ; Where } \gamma = \text{Atan2}\left[\frac{a_2S\theta_2}{(a_1+a_2C\theta_2}\right]$$

$$\frac{P_y}{\sqrt{A^2+B^2}} = \frac{A}{\sqrt{A^2+B^2}}S\theta_1 - \frac{B}{\sqrt{A^2+B^2}}C\theta_1 \qquad [3.9]$$

$$\frac{P_y}{\sqrt{A^2+B^2}} = S(\gamma + \theta_1) \text{ ; Where } \gamma = \text{Atan2}\left[\frac{a_2S\theta_2}{(a_1+a_2C\theta_2}\right]$$

$$\frac{P_y}{P_x} = \text{Tan}(\gamma + \theta_1) \text{ ; Where } \gamma = \text{Tan2}\left[\frac{a_2S\theta_2}{(a_1+a_2C\theta_2}\right]$$

$$\theta_1 = \text{Atan2}\left(\frac{P_y}{P_x}\right) - \text{Atan2}\left[\frac{a_2S\theta_2}{(a_1+a_2C\theta_2}\right]$$

$$\begin{cases} \boldsymbol{\theta_1 = Atan2\left(\frac{Y}{X}\right) - Atan2\left[\frac{a_2 Sin(\theta_2)}{(a_1 + a_2 Cos(\theta_2)}\right]} \\ \boldsymbol{\theta_2 = Atan2\left[\frac{X^2 + Y^2 - ({a_1}^2 + {a_2}^2)}{2a_1 a_2}\right]} \end{cases}$$

III.4 direct kinematic model of the SCARA robot

The direct kinematic model is given by equation [2.22]:

$$\dot{\mathbf{X}} = \mathbf{J}(\mathbf{q})\dot{\mathbf{q}}$$

With $\mathbf{J}(\mathbf{q}) \in \mathbf{R}^{\mathbf{m}\times\mathbf{n}}$ is the Jacobean matrix.

A partir des expressions [3.6], on note :

$$f_1 = \mathrm{P_x} = \mathrm{a_1 C\theta_1 + a_2 C(\theta_1 + \theta_2)} \quad [3.10]$$

$$f_2 = \mathrm{P_y} = \mathrm{a_1 S\theta_1 + a_2 S(\theta_1 + \theta_2)} \quad [3.11]$$

$$f_2 = \mathrm{P_z} = \mathrm{d_3} \quad [3.12]$$

The Jacobean matrix is: $$\mathbf{J(q)} = \begin{bmatrix} \frac{\partial \mathbf{f_1}}{\partial \boldsymbol{\theta_1}} & \frac{\partial \mathbf{f_1}}{\partial \boldsymbol{\theta_2}} & \frac{\partial \mathbf{f_1}}{\partial \mathbf{d_3}} \\ \frac{\partial \mathbf{f_2}}{\partial \boldsymbol{\theta_1}} & \frac{\partial \mathbf{f_2}}{\partial \boldsymbol{\theta_2}} & \frac{\partial \mathbf{f_2}}{\partial \mathbf{d_3}} \\ \frac{\partial \mathbf{f_3}}{\partial \boldsymbol{\theta_1}} & \frac{\partial \mathbf{f_3}}{\partial \boldsymbol{\theta_2}} & \frac{\partial \mathbf{f_3}}{\partial \mathbf{d_3}} \end{bmatrix} \quad [3.13]$$

By derivation of expressions [3.6], we obtain:

$$\mathbf{J(q)} = \begin{bmatrix} \mathbf{-a_1 S\theta_1 - a_2 S(\theta_1 + \theta_2)} & \mathbf{- a_2 S(\theta_1 + \theta_2)} & \mathbf{0} \\ \mathbf{a_1 C\theta_1 + a_2 C(\theta_1 + \theta_2)} & \mathbf{a_2 C(\theta_1 + \theta_2)} & \mathbf{0} \\ \mathbf{0} & \mathbf{0} & \mathbf{1} \end{bmatrix} \quad [3.14]$$

So the direct kinematic model is expressed as follows:

$$\dot{\mathbf{X}} = \frac{\mathbf{dx}}{\mathbf{dt}} = \begin{bmatrix} \mathbf{V_x} \\ \mathbf{V_y} \\ \mathbf{V_z} \end{bmatrix} = \begin{bmatrix} \mathbf{-a_1 S\theta_1 - a_2 S(\theta_1 + \theta_2)} & \mathbf{- a_2 S(\theta_1 + \theta_2)} & \mathbf{0} \\ \mathbf{a_1 C\theta_1 + a_2 C(\theta_1 + \theta_2)} & \mathbf{a_2 C(\theta_1 + \theta_2)} & \mathbf{0} \\ \mathbf{0} & \mathbf{0} & \mathbf{1} \end{bmatrix} \begin{Bmatrix} \dot{\boldsymbol{\theta}}_1 \\ \dot{\boldsymbol{\theta}}_2 \\ \dot{\mathbf{d}}_3 \end{Bmatrix} \quad [3.15]$$

So

$$\mathbf{V_x} = [-\mathbf{a_1 S\theta_1} - \mathbf{a_2 S(\theta_1 + \theta_2)}]\dot{\boldsymbol{\theta}}_1 - \mathbf{a_2 S(\theta_1 + \theta_2)}\dot{\boldsymbol{\theta}}_2$$

$$\mathbf{V_y} = [\mathbf{a_1 C\theta_1} + \mathbf{a_2 C(\theta_1 + \theta_2)}]\dot{\boldsymbol{\theta}}_1 + \mathbf{a_2 C(\theta_1 + \theta_2)}\dot{\boldsymbol{\theta}}_2$$

$$\mathbf{V_z} = \dot{\mathbf{d}}_3$$

III.5 Invers kinematic model of the SCARA robot

The inverse kinematic model is given by equation [2.24]:

$$\dot{\mathbf{q}} = \mathbf{J}^{-1}\,\dot{\mathbf{X}}$$

$$\begin{bmatrix} \dot{\boldsymbol{\theta}}_1 \\ \dot{\boldsymbol{\theta}}_2 \\ \dot{\mathbf{d}}_3 \end{bmatrix} = \begin{bmatrix} \dfrac{\mathbf{C(\theta_1 + \theta_2)}}{\mathbf{a_1 S\theta_1}} & \dfrac{\mathbf{S(\theta_1 + \theta_2)}}{\mathbf{a_1 S\theta_1}} & \mathbf{0} \\ \dfrac{-\mathbf{a_2 C(\theta_1 + \theta_2) - a_1 C\theta_2}}{\mathbf{a_1 a_2 S\theta_1}} & \dfrac{-\mathbf{a_2 S(\theta_1 + \theta_2) - a_1 S\theta_2}}{\mathbf{a_1 a_2 S\theta_1}} & \mathbf{0} \\ \mathbf{0} & \mathbf{0} & \mathbf{1} \end{bmatrix} \begin{bmatrix} \dot{\mathbf{P}}_x \\ \dot{\mathbf{P}}_y \\ \dot{\mathbf{P}}_z \end{bmatrix}$$

$$\dot{\boldsymbol{\theta}}_1 = \frac{\boldsymbol{C(\theta_1 + \theta_2)}\dot{\boldsymbol{P}}_x + \boldsymbol{S(\theta_1 + \theta_2)}\dot{\boldsymbol{P}}_x}{\boldsymbol{a_1 S\theta_1}}$$

$$\dot{\boldsymbol{\theta}}_2 = \frac{[-\boldsymbol{a_2 C(\theta_1 + \theta_2) - a_1 C\theta_2}]\dot{\boldsymbol{P}}_y + [-\boldsymbol{a_2 S(\theta_1 + \theta_2) - a_1 S\theta_2}]\dot{\boldsymbol{P}}_y}{\boldsymbol{a_1 a_2 S\theta_1}}$$

$$\dot{\mathbf{d}}_3 = \dot{\boldsymbol{P}}_z$$

III.5 Conclusion:

We have presented in this chapter the mathematical tools used in robotics to find the geometric model, the kinematic model of SCARA robot RRPR type.

We have been able to arrive at the coordinates of the end-effector position and the equations of the angle position, and then we were also able to determine operational velocity and joint velocity equations.

CHAPITRE IV:

DESIGN AND REALIZATION OF SCARA ROBOT

IV.1 Introduction

We are in the process of manufacturing our SCARA robot, which will be operated using an Arduino Uno. This chapter will be structured into three sections. The first part will primarily focus on the design phase utilizing CATIA V5. The second part will cover the robot components, assembly, and drafting. Lastly, the third part will involve simulating the performance of our SCARA robot.

IV.2 Design and manufacture of SCARA robot parts:

IV.2.1 Design with CATIA V5:

CATIA V5, which is developed by Dassault Systèmes in France, is an advanced suite of CAD/CAM/CAE software solutions for Product Lifecycle Management. CATIA V5 offers the advantage of minimizing the learning curve by providing the flexibility to employ feature-based and parametric designs. Apart from creating solid models, sheet metal components, and assemblies, CATIA also enables the generation of 2D drawing views through its Drafting workbench.[18].

IV.2.2 Parts design:

Parts are the fundamental building blocks of an object or product. When working with CATIA V5, parts serve as initial components in the creation process. As CATIA V5 is primarily designed for 3D modeling, all parts generated in the software are in 3D format. Additionally, each part can be assigned a specific material type, providing more detail and precision to the virtual representation.

Table IV.1:SCARA robot parts in real and design

Real parts	Design parts by CATIA V5
a. **body** 	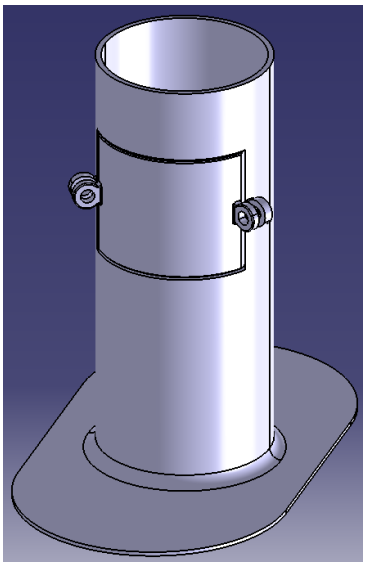
b. **Arm I** 	
c. **Arm II** 	
d. **Rod bearing I** 	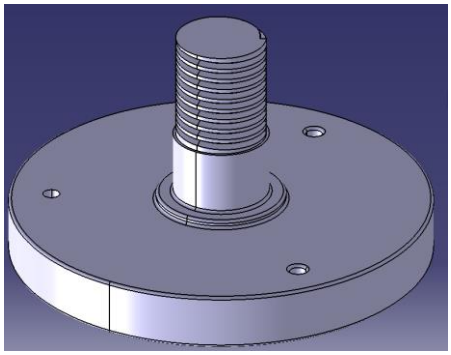

e. Bearing housing I

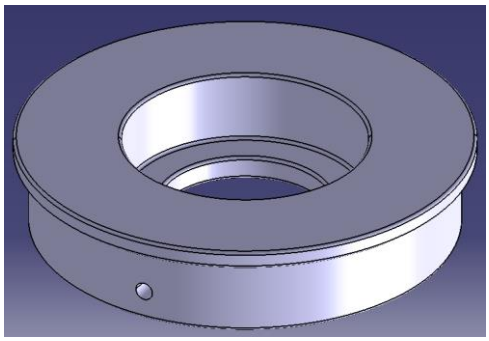

f. Rod bearing II

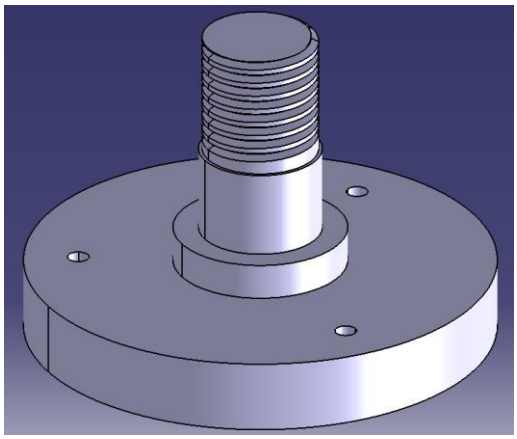

g. Bearing housing II

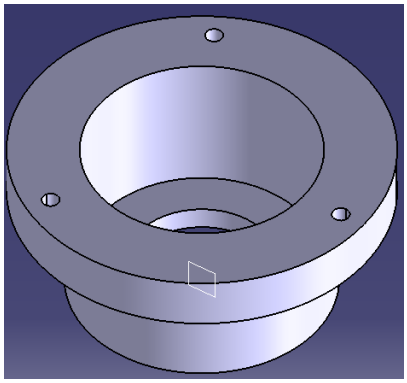

h. Nuts

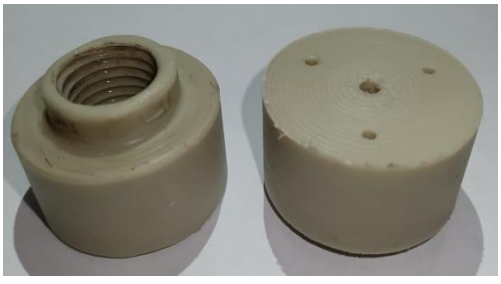

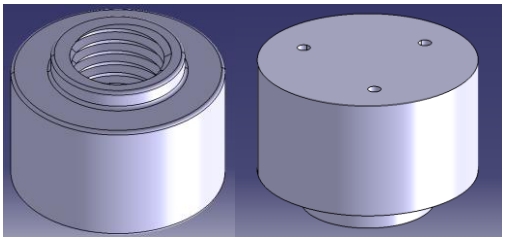

IV.2.3 The Assembly modeling:

Assembly modeling is a technique applied by CAD and product visualization software systems to utilize multiple files that shows components within a product. The components within an assembly are called as solid / surface models. The personal data files defining the 3D geometry of personal components are assembled together via a number of sub assembly levels to generate an assembly explaining the complete product [19].

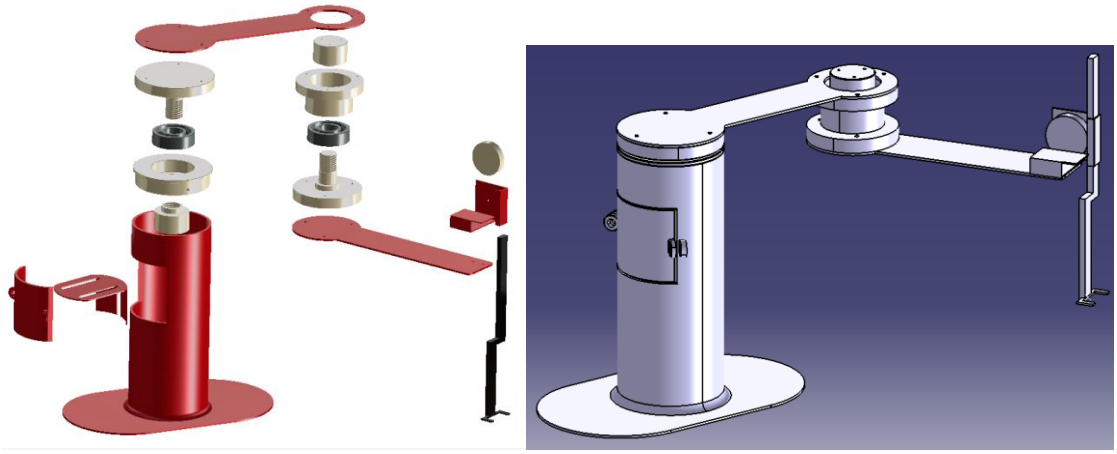

Figure IV.1 : Assembly Scara robot

IV.2.4 The Drafting:

Drafting is the procedure of producing drawings that effectively communicate how something can be constructed. It involves presenting a 3D object on a 2D sheet of paper, illustrating its appearance and details from various viewpoints. Through drafting, technical professionals enhance the comprehensibility of a design by utilizing symbols, lines, and curves in a drawing. This process facilitates the transfer of the designer's concept to manufacturers or laborers, enabling clear understanding and implementation of the intended design. [20].

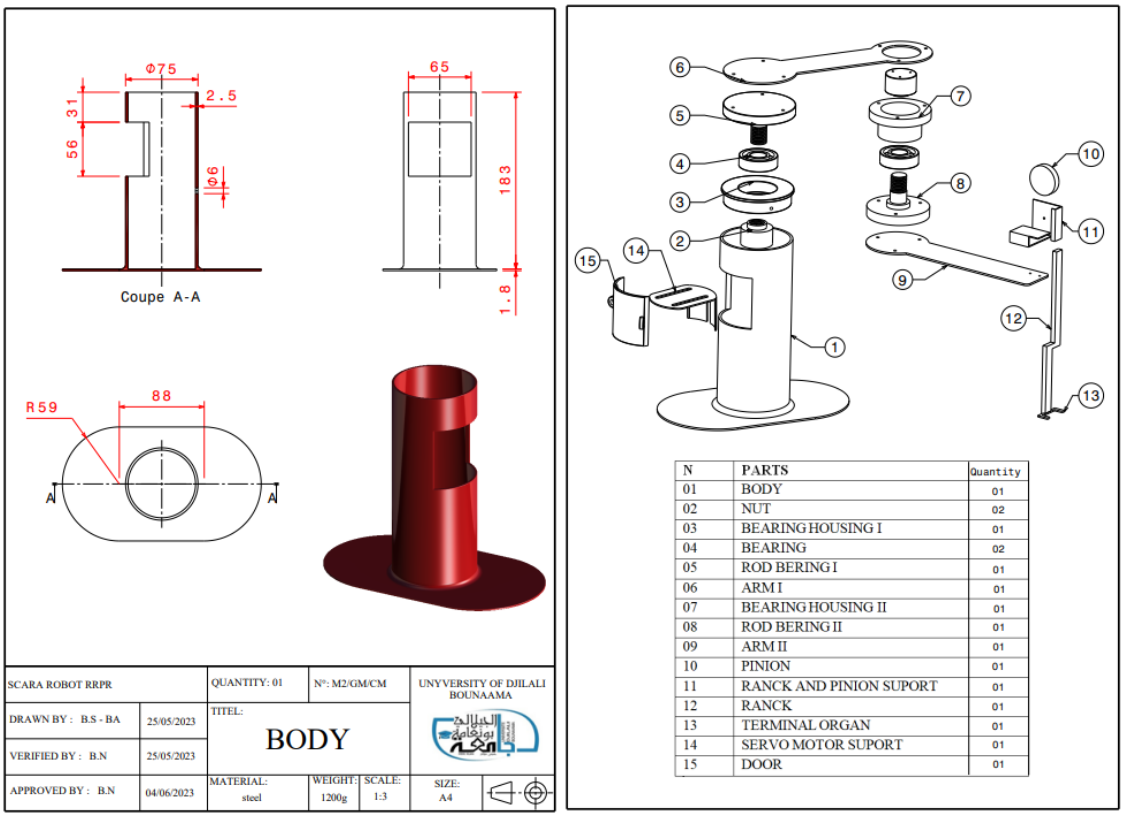

N	PARTS	Quantity
01	BODY	01
02	NUT	02
03	BEARING HOUSING I	01
04	BEARING	02
05	ROD BERING I	01
06	ARM I	01
07	BEARING HOUSING II	01
08	ROD BERING II	01
09	ARM II	01
10	PINION	01
11	RANCK AND PINION SUPORT	01
12	RANCK	01
13	TERMINAL ORGAN	01
14	SERVO MOTOR SUPORT	01
15	DOOR	01

Figure IV. 2: Body drafting and exploded view drawing (Drafting of all parts in appendix)

IV.3 Robot components :

The SCARA robot is composed of two arms constructed from galvanized sheet metal. The actuator employed in this robot is a Servomotor. The machined parts within the robot are made from plastic material. The various components of the SCARA robot are listed as follows:

IV.3.1 Components made with machining

List of Components made by a lathe:

1. Rod bearing I
2. Bearing housing I
3. Rod bearing II
4. Bearing housing II
5. Nuts

Figure IV. 3: Manufacturing step in the lathe machine

List of Components made by a Hydraulic Sheet Metal Bending Machine:

1. Servo motor fixature
2. Ranck and Pinion Suppor

Figure IV.4: Manufacturing step in the Hydraulic Sheet Metal Bending Machine

IV.3.2 Mechanical Components:

IV.3.2.1 Bearings

The function of a bearing is to allow two elements to be in rotation relative to each other with precision and with optimized friction, replacing a slip by a bearing [21].

A ball bearing is a type of rolling-element bearing that serves three main functions while it facilitates motion: it carries loads, reduces friction and positions moving machine parts. Ball bearings use balls to separate two “races,” or bearing rings, to reduce surface contact and friction across moving planes [22].

Figure IV. 5: Boll bearings

For our system we needed one size of ball bearing as explained in the table below.

Table IV.2: The specifications of bearing

	Quantity	Inner diameter (mm)	Outside diameter (mm)	Thickness (mm)
Size	2	17	40	12

IV.3.2.2 Rack and Pinion

Rack and pinion, a mechanical device consisting of a bar of rectangular cross-section (the rack), having teeth on one side that mesh with teeth on a small gear (the pinion). The pinion may have straight teeth [23].

Figure IV.6: Rack and Pinion

IV.3.3 Electronic components

IV.3.3.1 Servo motor

A servo motor is a linear actuator or rotary actuator that provides precise control of linear or angular position, acceleration, and speed. It consists of a motor coupled to a position feedback sensor. It also requires a relatively sophisticated controller, often a dedicated module designed specifically for use with servo motors [24].

In this project used three types of servo motors which are the **SG90, MG90S** and the **MG996R**.

1. This High-Torque MG996R Digital Servo features metal gearing resulting in extra high 10kg stalling torque in a tiny package. The MG996R is features upgraded shock-proofing and a redesigned PCB and IC control system that makes it much more accurate than its predecessor.

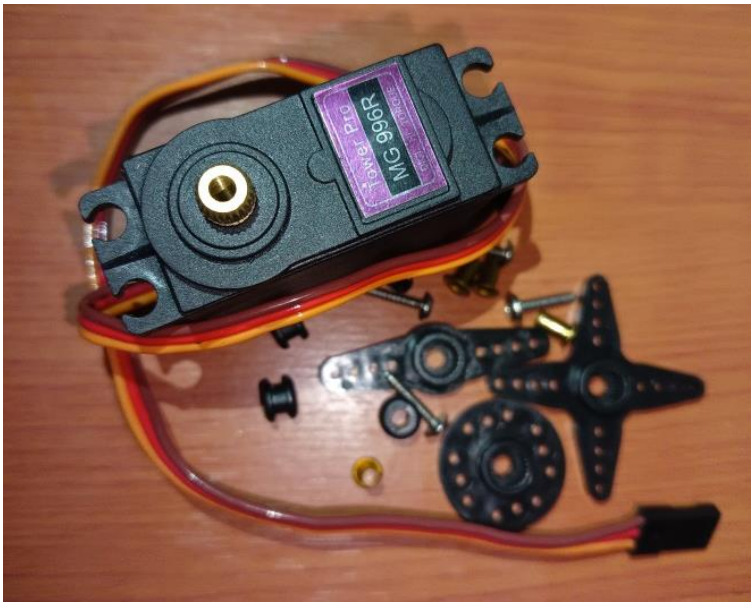

Figure IV. 7: Servo motor MG996R

The specifications for the servomotors are detailed in the table provided below.

Table IV.3: The specifications of the MG996R servomotor

weight	55g
Stall torque	9.4kgf.cm(4.8V) - 11kgf.cm(6V)
Operating speed	0.17s/60°(4.8V) - 0.14s/60°(6V)
Operating voltage	4.8V a 7.2V
Runninig current	500mA - 900mA
Type of gear	metal
Temperature range	0°C – 55°C

2. SG90 Servo motor

Figure IV.8: Servo motor SG90

The specifications for the servomotor are detailed in the table provided below.

Table IV. 4: The specifications of the SG90 servomotor

weight	9g
Stall torque	1.8kgf.cm
Operating speed	0.12sec/60°
Operating voltage	4.8V
Type of gear	plastic

3. MG90S is a micro servo motor with metal gear. This small and lightweight servo comes with high output power, thus ideal for RC Airplane, Quadcopter or Robotic Arms.

Figure IV. 9: Servo motor MG90s

The specifications for the servomotor are detailed in the table provided below.

Table IV. 5: The specifications of the MG90S servomotor.

weight	13.4g
Stall torque	2.2 kg/cm (6V)
Operating speed	0.1s/60° (4.8V)
Operating voltage	4.8V to 6V (Typically 5V)
Runninig current	500mA - 900mA
Type of gear	metal

IV.3.3.2 Arduino Uno

A microcontroller board called Arduino Uno is based on the ATmega328P (datasheet). It contains a 16 MHz ceramic resonator (CSTCE16M0V53-R0), 6 analog inputs, 14 digital input/output pins (of which 6 may be used as PWM outputs), a USB port, a power connector, an ICSP header, and a reset button. It comes with everything

required to support the microcontroller; to get started, just use a USB cable to connect it to a computer, or an AC-to-DC converter or battery to power it. You can experiment with your Uno without being very concerned that you'll make a mistake; in the worst case, you can replace the chip for a few dollars and start over[25].

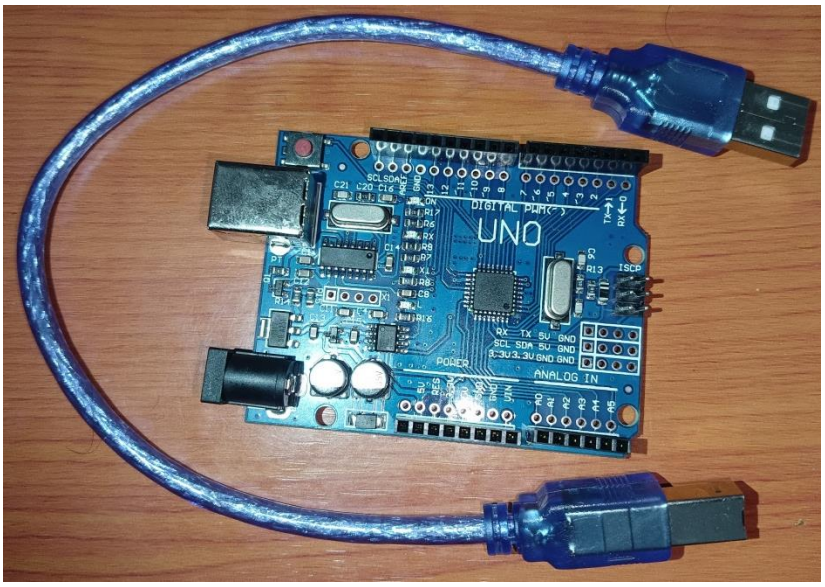

Figure IV. 10: Arduino Uno board

Table IV. 6: The specifications of the ARDUNO UNO

Microcontroller	ATmega328P
Operating Voltage	5V
Input Voltage (recommended)	7-12V
Input Voltage (limit)	6-20V
Digital I/O Pins	14 (of which 6 provide PWM output)
PWM Digital I/O Pins	6
Analog Input Pins	6
DC Current per I/O Pin	20 mA
DC Current for 3.3V Pin	50 mA
Flash Memory	32 KB (ATmega328P) of which 0.5 KB used by bootloader
SRAM	2 KB (ATmega328P)

EEPROM	1 KB (ATmega328P)
Clock Speed	16 MHz
LED_BUILTIN	13
Length	68.6 mm
Width	53.4 mm
Weight	25 g

IV.3.3.3 HC-05 Bluetooth Module

Simple AT commands may be used to select the software-configurable Master/Slave mode of this Bluetooth module. The straightforward substitute for wired serial connections is this module. You may use it to link MCU, GPS, and robot-like devices to a PC or embedded board by simply transforming a standard serial port into a wireless serial port. This module has a built-in 3.3V regulator, but it can also be powered by a 3.6V–6V supply. Since the RXD and TXD pins are at 3.3V level, use a MAX3232 to connect it to the PC serial port. The status LED onboard is there. The 1234 default pairing password [26].

Figure IV. 11: HC-05 BLUETOOTH MODULE

IV.3.3.4 Jumper wires

Jumpers are typically small metal connections that are used to open or close circuit components. They have two or more connecting points that control a circuit board for an electrical system. They have connection pins at either end and are electrical cables. They are employed to connect two circuit locations without the usage of solder.

Male-to-male jumper, Male-to-female jumper, and Female-to-female jumper are the three varieties that are available [27].

Figure IV. 12: Male-to-male and Female-to-female jumper

IV.3.3.5 The breadboard

The breadboard is a circuit construction technique that is designed to allow the rapid creation of circuits without the need for soldering or making permanent connections [28].

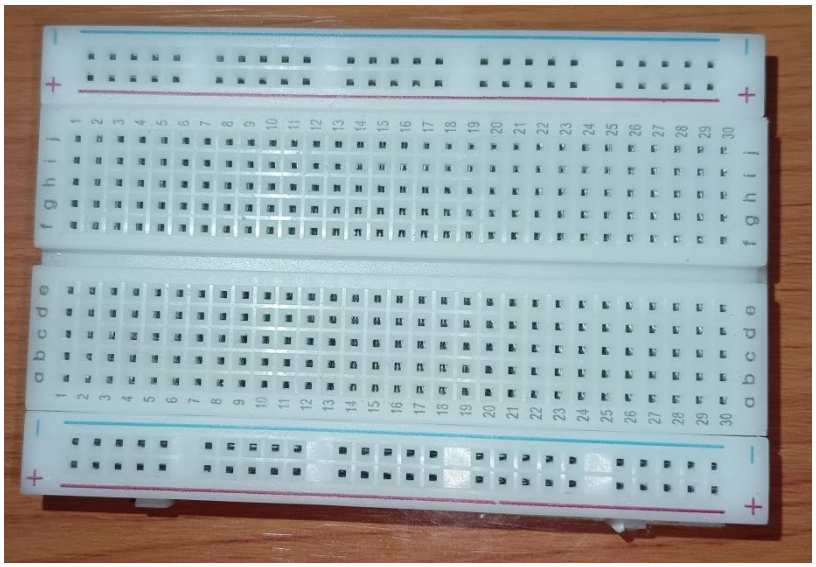

Figure IV. 13: The breadboard

IV.3.3.6 Power Supply and electronic circuitry

The operating voltage of the Arduino board is +5v. This can be easily supplied by using the USB cable connected to the computer. Each individual servo also requires voltage supply of +5v.

With the Tinkercad site [30] we were able to try the connection of the different components in (**Figure IV.41**).

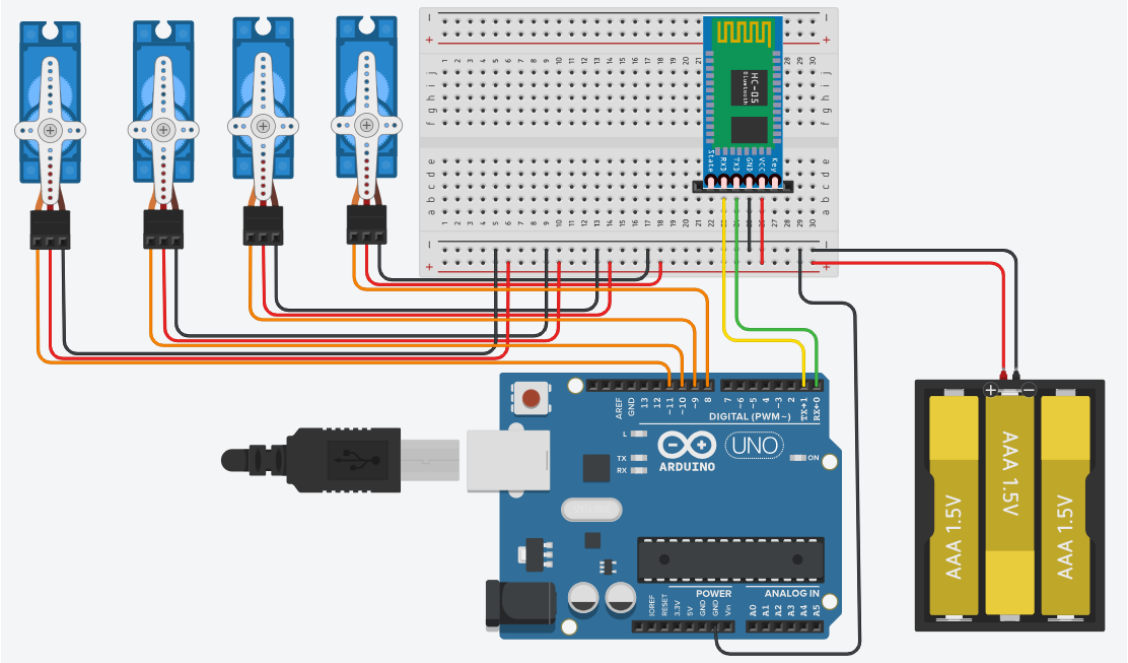

Figure IV. 14: Schematic diagram of Arduino connection

IV.3.3.7 Arduino program

The Arduino Software (IDE) makes it easy to write code and upload it to the board offline. This software can be used with any Arduino board [25].

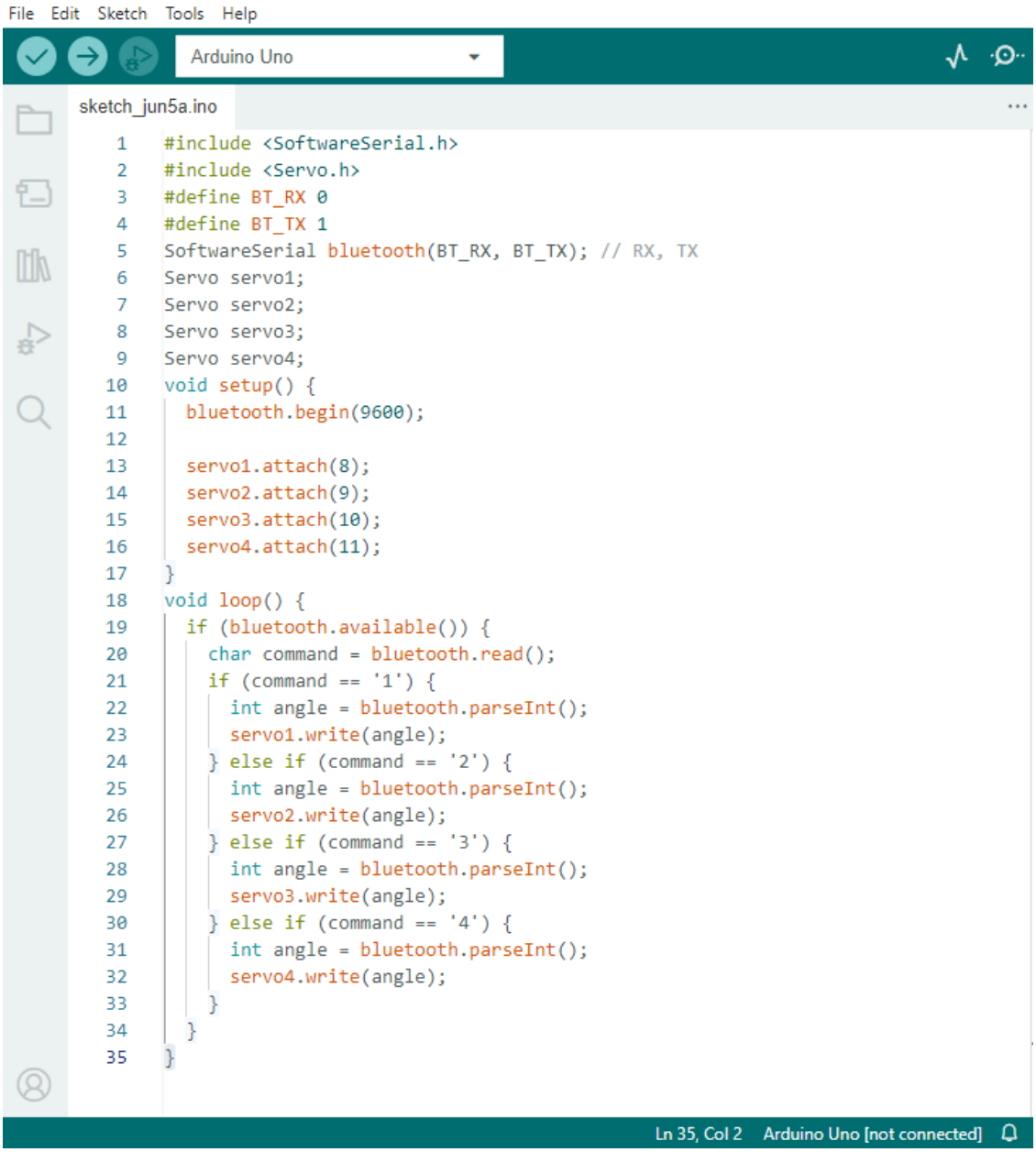

Figure IV. 15: Arduino program

IV.3.4 Assembly of the Scara Robot:

After the realization of the different parts of the Scara robot, we moved on to the final assembly and the incorporation of those components, we wired them with the Arduino using cables. The following figure illustrates the final assembly of our Scara robot and the number of articulations. (Figure IV.16)

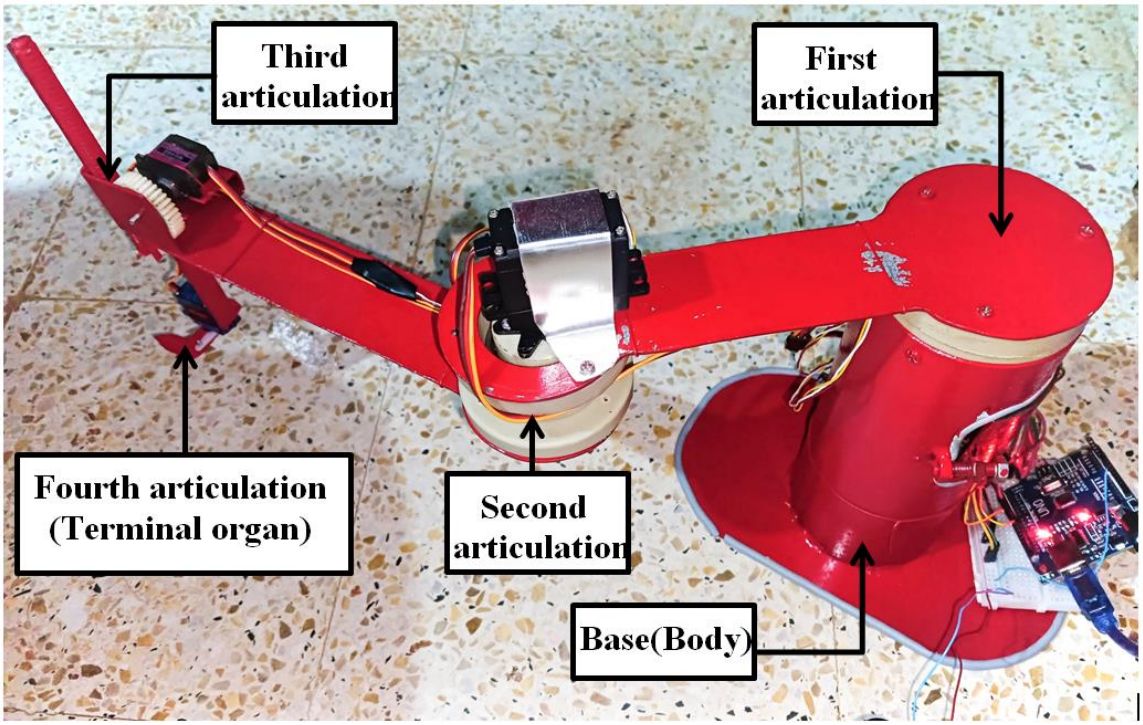

Figure IV. 16: Assembly final of the Scara Robot

IV.4 Imposed trajectory made with our Scara robot:

Our robot is a four degree-of-freedom, (Figure IV.17). The first joints is located at the base(body) of the robot, Joint 2 is located along a link 160mm from the first joints

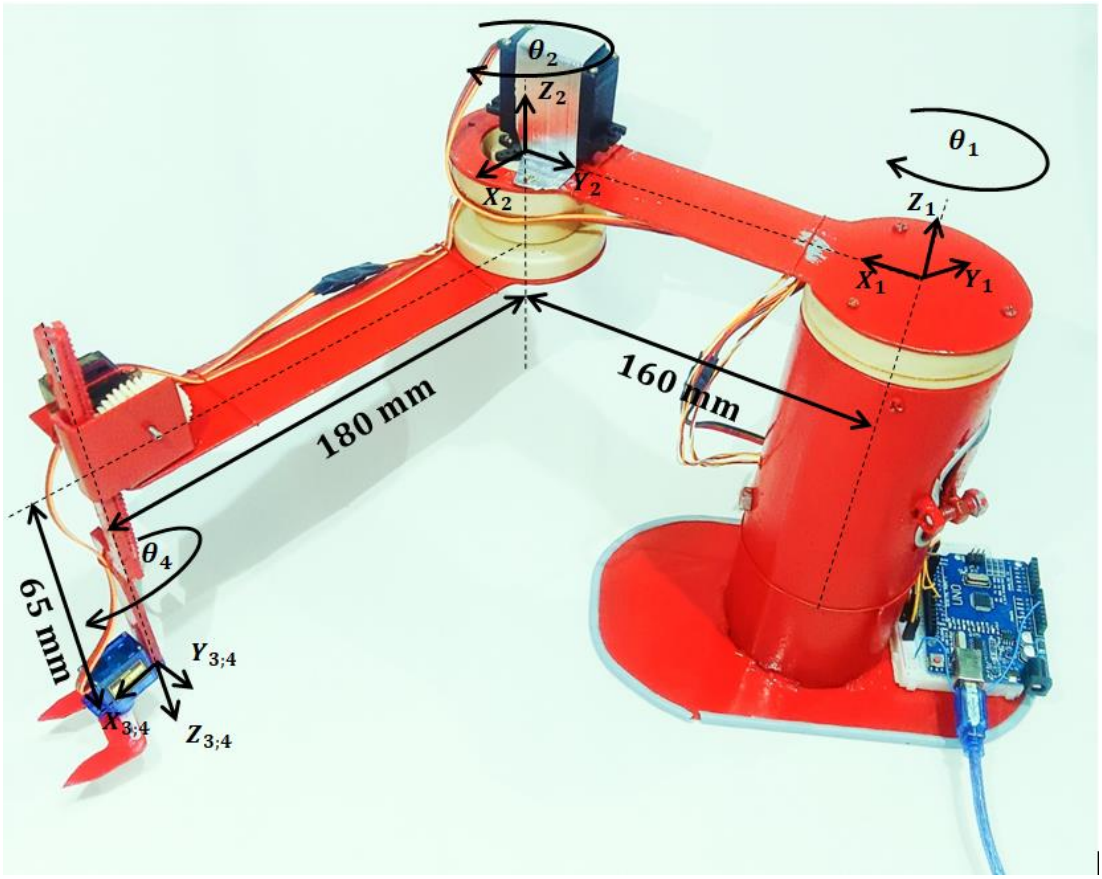

Figure IV. 17: The Scara Robot axes

The kinematic model with frame assignments according to the Denavit-Hartenberg (D-H) notations. The kinematic parameters according to this model are given in Table IV.7.

Table IV. 7 Denavit Hartenberg (D-H) of our robot

i	a_i	α_i	d_i	θ_i
1	160	0°	0	θ_1
2	180	180°	0	θ_2
3	0	0°	d3	0°
4	0	0°	0	θ_4

Where the joint limits are:

$-90^o \leq \theta_1 \leq 90^o$; $-90^o \leq \theta_2 \leq 90^o$; $0 \leq d_3 \leq 65$mm; $-90^o \leq \theta_4 \leq 90^o$

The manipulator robot must follow a trajectory that passes through eight waypoints (Table IV.8) from equation [3.6].

Table IV. 8: **Our robot waypoints**

	Px(mm)	Py(mm)	Pz(mm)	θ_1(deg)	θ_2(deg)	d_3(mm)
1	31	-337	-60	-90	10	60
2	211	-240	-65	-70	40	65
3	308	-61	-63	-35	45	63
4	292	23	-62	-28	61	62
5	248	128	-60	-10	70	60
6	0	270	-59	50	75	59
7	138	291	-20	45	37	20
8	234	191	-21	10	55	21

IV.5 Simulation of our SCARA robot trajectory

IV.5.1 Joint position

For our robot, the joint position can be calculated for 3 joints. The robot's first and second joints can rotate at a maximum angle of -90 to 90 degrees. while the third joint has a linear movement of 65 mm. In order to compare the results, we analyzed using two different software, CATIA V5 and Matlab.

In the beginning, we used CATIA software to create a path that passes through the eight points given in the (Table IV.8), In addition, we created a simulation by having our robot follow that path at the time T=5.2s. And according to the Matlab software, we made a simulation using the equation [3.6]. and (Table IV.8). The results are shown in the graphs following.

In (Figure IV. 18) by CATIA software shows the first joint position graph in degrees as a function of time, while (Figure IV. 19) by Matlab shows the same graph, Comparing the two graphs also reveals that they respect the requirement of passing through the maximum and lowest degrees of the angle while traversing all of the points in the table.

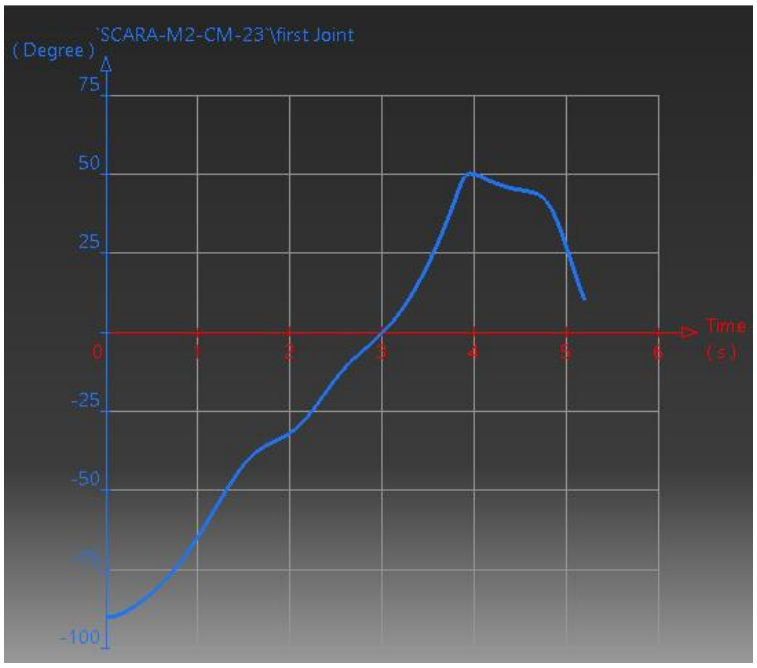

Figure IV. 18 First joint position with CATIA V5

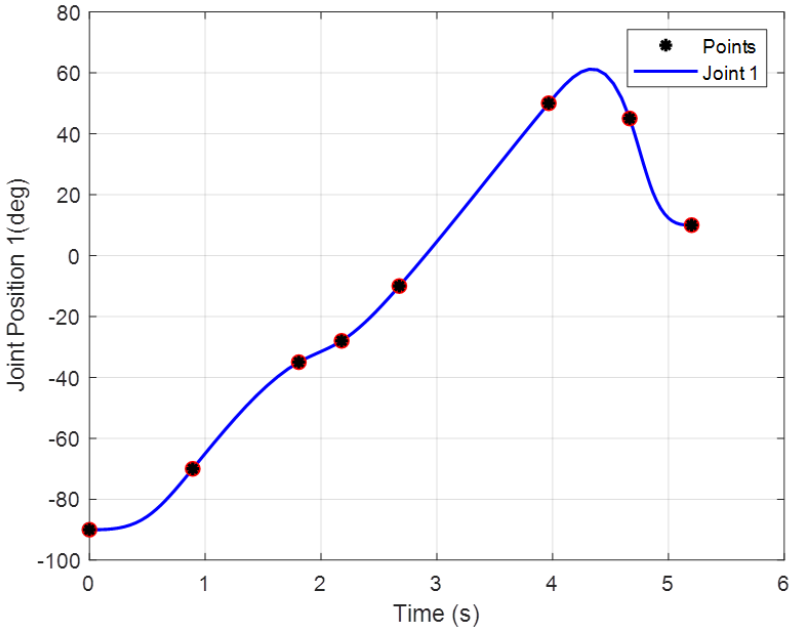

Figure IV. 19 First joint position with Matlab

Also in (Figure IV. 20) by CATIA software shows the second joint position graph in degrees as a function of time, while (Figure IV. 21) by Matlab shows the same graph, When comparing the two graphs, we see that the second arm follows the same angle to arrive at the table's x and y coordinates.

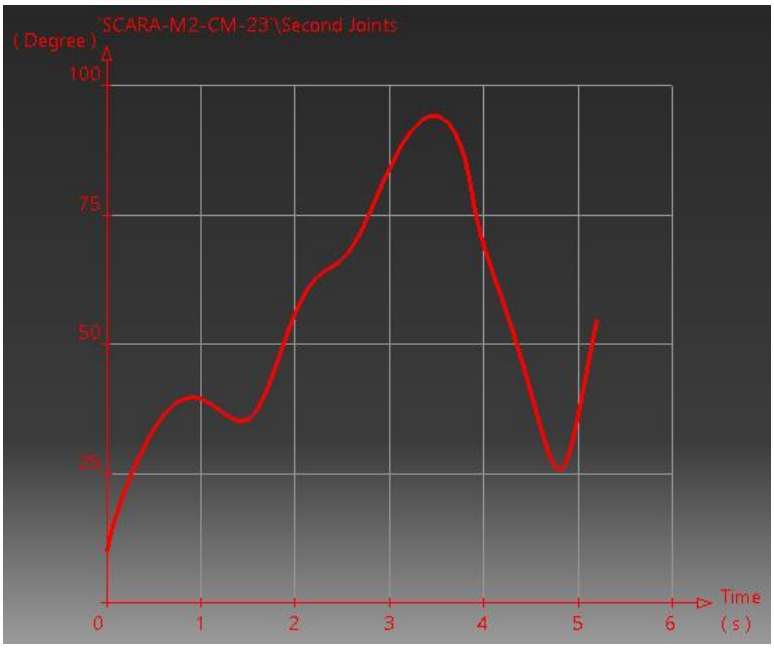

Figure IV. 20 Second joint position with CATIA V5

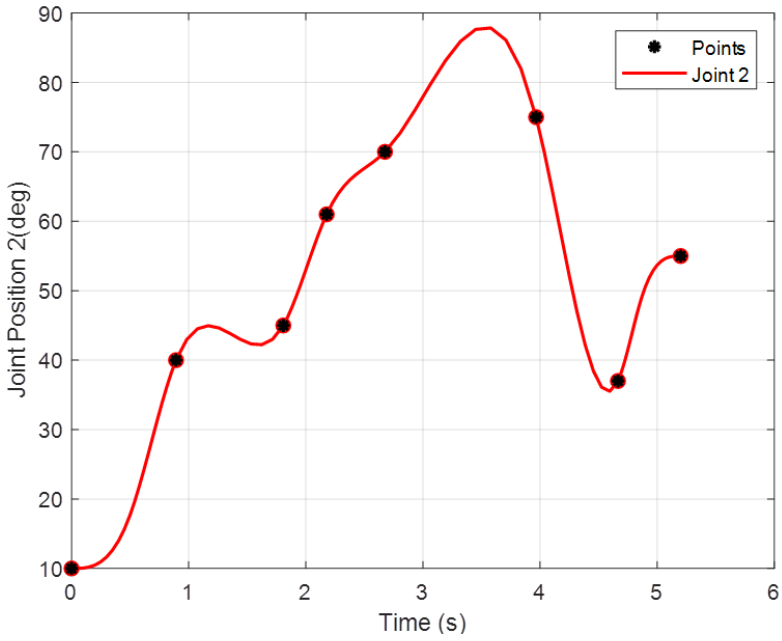

Figure IV. 21 Second joint position with Matlab

The third joint position graph in millimeters as a function of time is shown in (Figure IV.22) using CATIA software, and the same graph is also shown in (Figure IV.23) by Matlab.

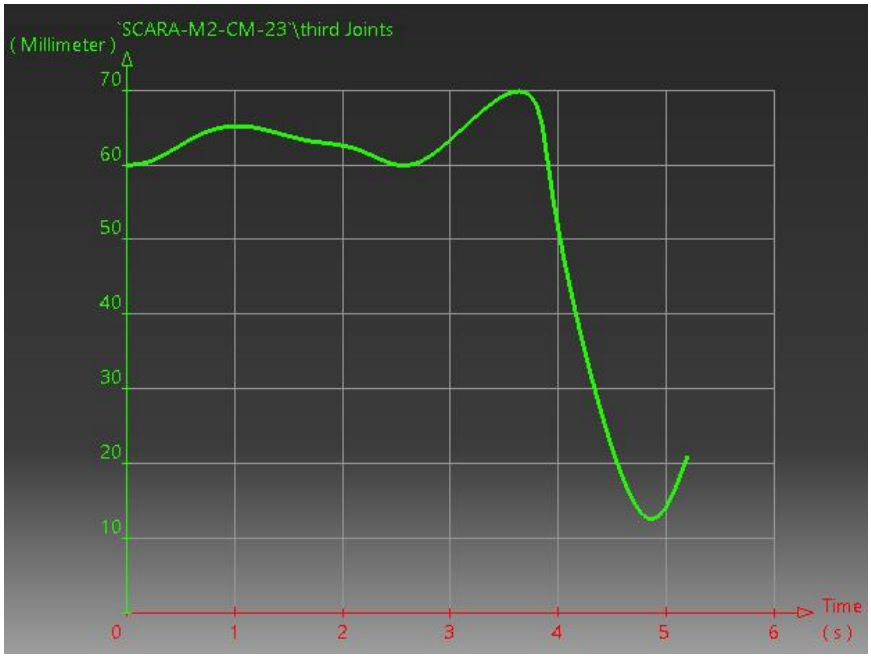

Figure IV. 22 Third joint position with CATIA V5

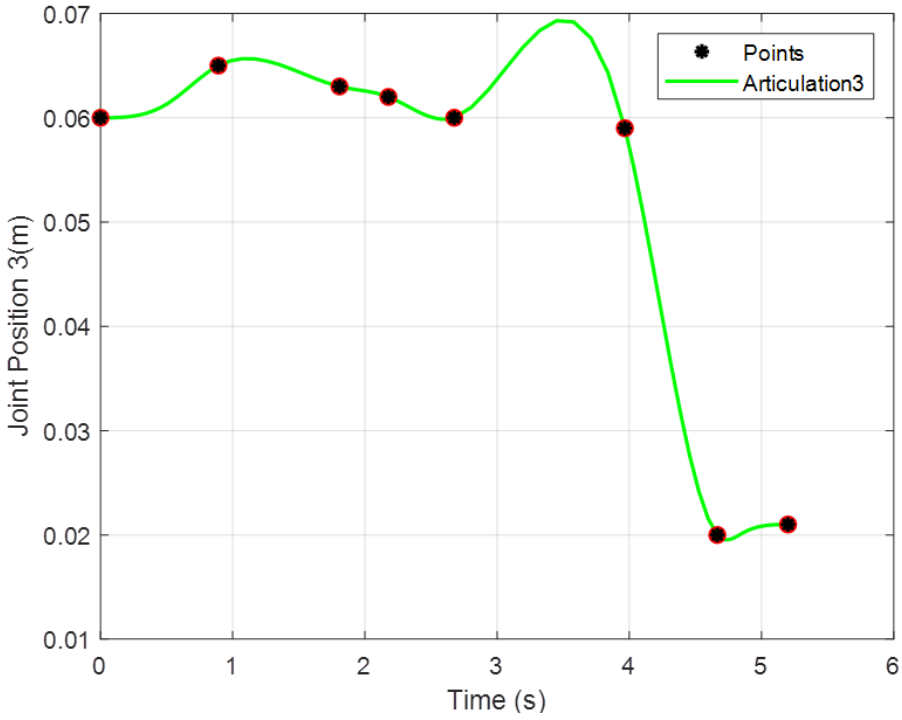

Figure IV. 23 Third joint position with Matlab

The two software programs gave the same results, so we can conclude that this trajectory can be reached by our robot.

IV.5.2 motion specification

Matlab, a simulation of the Scara robot is created, as seen in (Figure IV.24). The robot may be moved and connection settings can be adjusted using the GUI window interface.

The following figures show our robot passing from the first point to the final point through the via-points using cubic spline functions.

In (Figure IV.24) displays our robot at the initial position Px=31mm, Py=337mm, Pz=-60mm at time 0 s, with the first joint at an angle of -90 degrees, the second joint at a 10 degree angle, and the third joint at d3=60 mm. The first picture was created with CATIA, while the second one with Matlab.

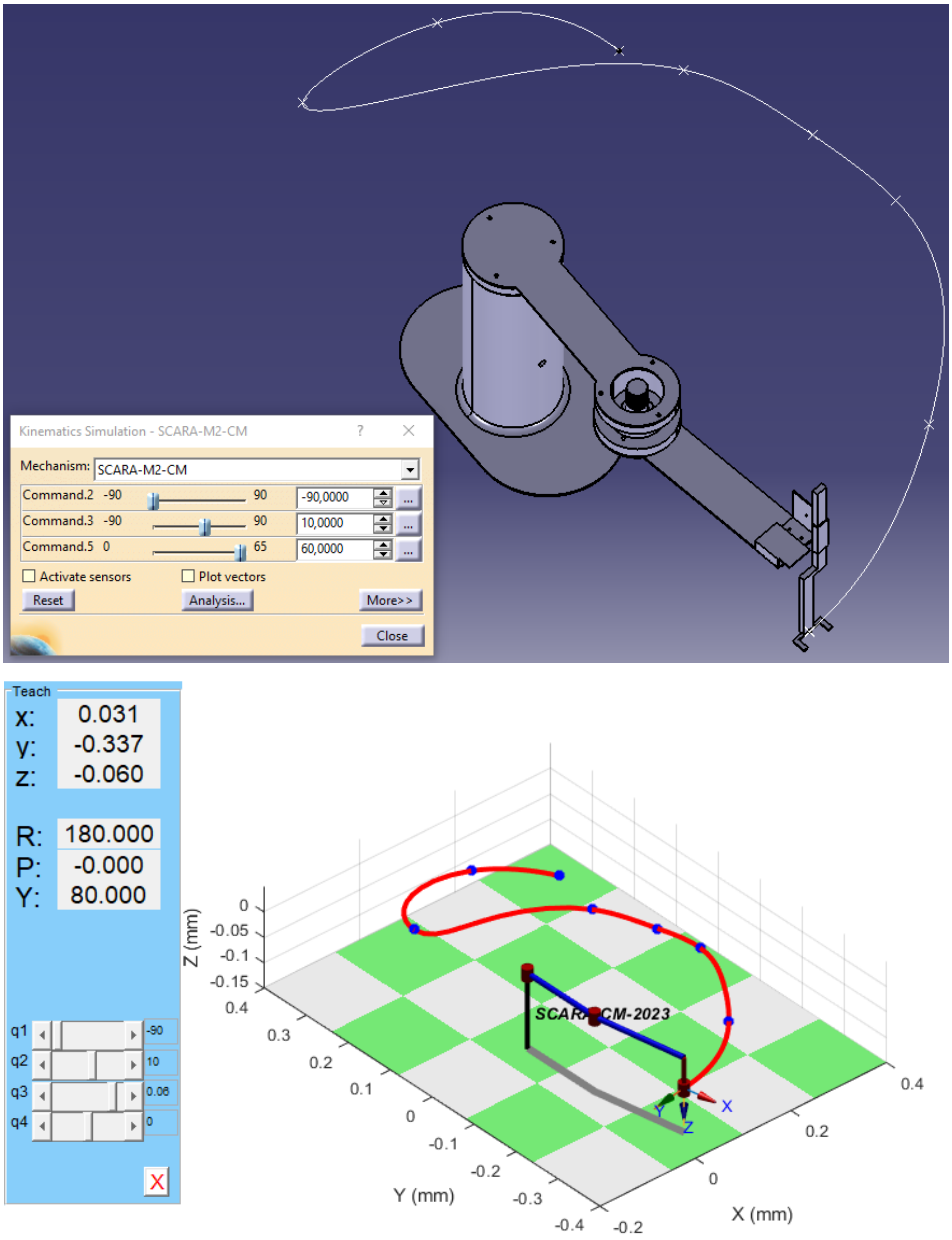

Figure IV. 24 First waypoint position with CATIA V5 and Matlab

In (Figure IV.25) displays our robot at the second position Px=211mm, Py=-240mm, Pz=-65mm at time 0.8920 s, with the first joint at an angle of -70 degrees, the second joint at a 40 degree angle, and the third joint at d3=65 mm. The first picture was created with CATIA, while the second one with Matlab

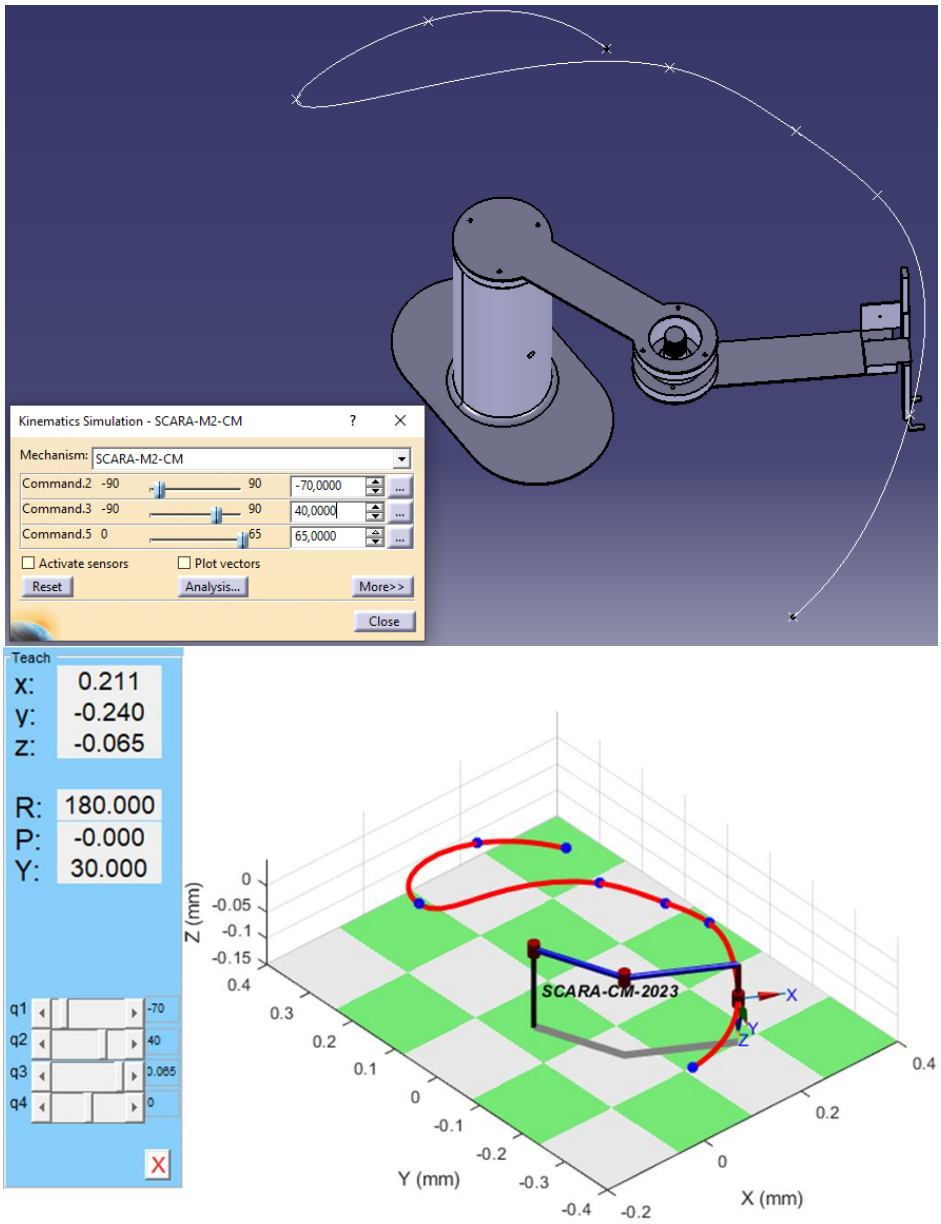

Figure IV. 25 Second waypoint position with CATIA V5 and Matlab

In (Figure IV.26) the same description as the first and second description, while the position of the robot changes to the third point Px=308mm, Py=-61mm, Pz=-63mm at time 1.8080 s , with the first joint at an angle of -35 degrees, the second joint at a 45 degree angle, and the third joint at d3=63 mm

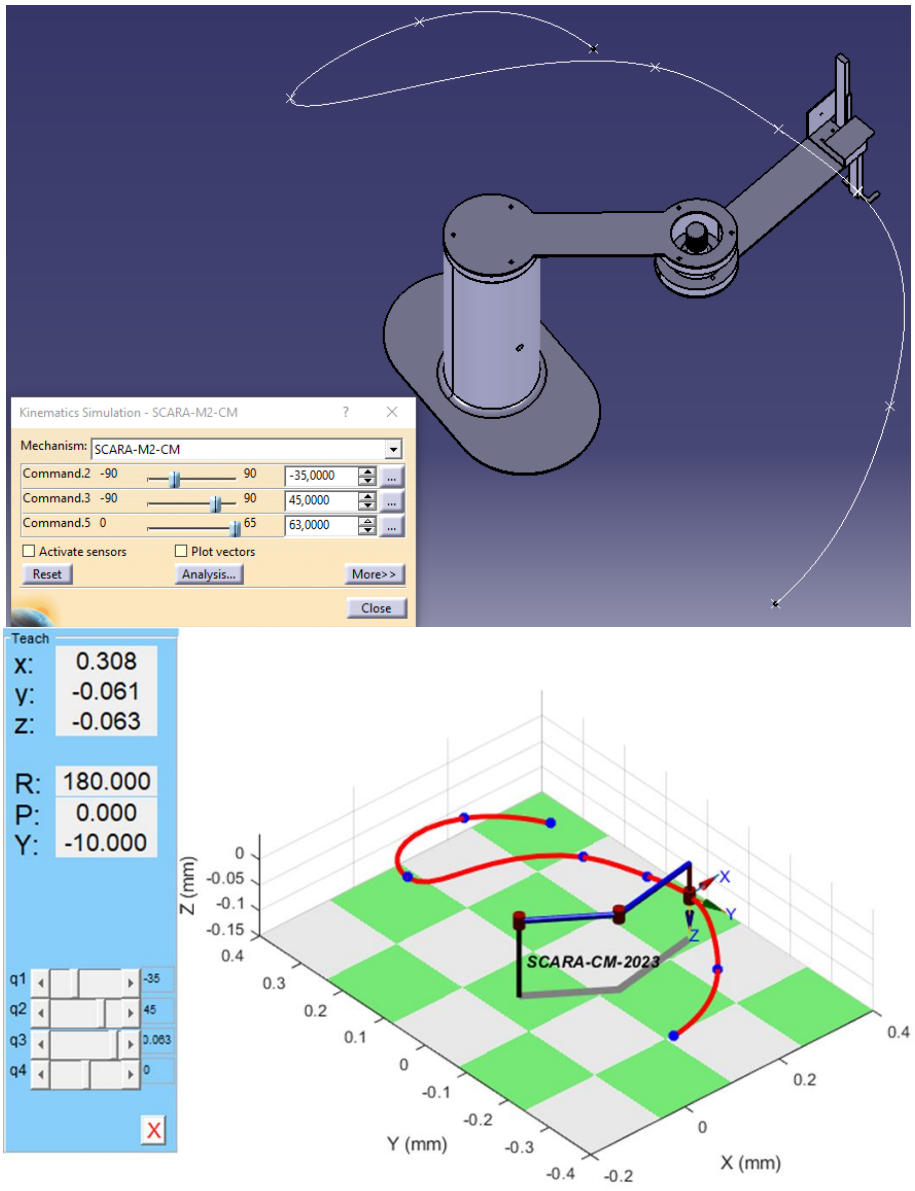

Figure IV. 26 Third waypoint position with CATIA V5 and Matlab

In (Figure IV.27) displays the position of the robot changes to the fourth point Px=292mm, Py=23mm, Pz=-62mm at time 2.1780 s, with the first joint at an angle of -28 degrees, the second joint at a -61 degree angle, and the third joint at d3=62 mm

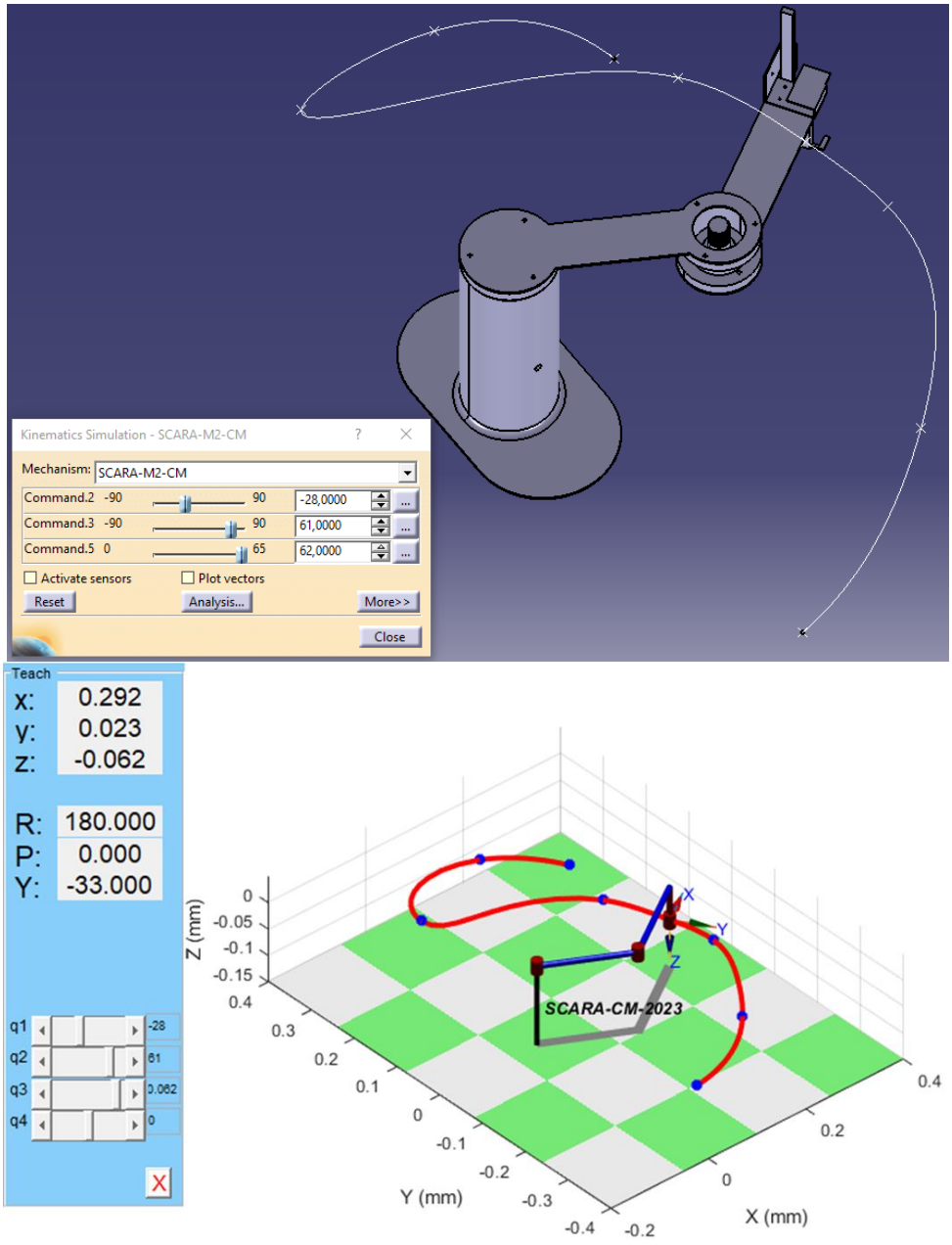

Figure IV. 27 Fourth waypoint position with CATIA V5 and Matlab

The robot's position is altered at the sixth point of (Figure IV.28), where the new coordinates are Px=248 mm, Py=128 mm, and Pz=-60 mm at time 2.6760 s. The first joint is at a -10 degree angle, the second is at a 70 degree angle, and the third is at a d3=60 mm angle.

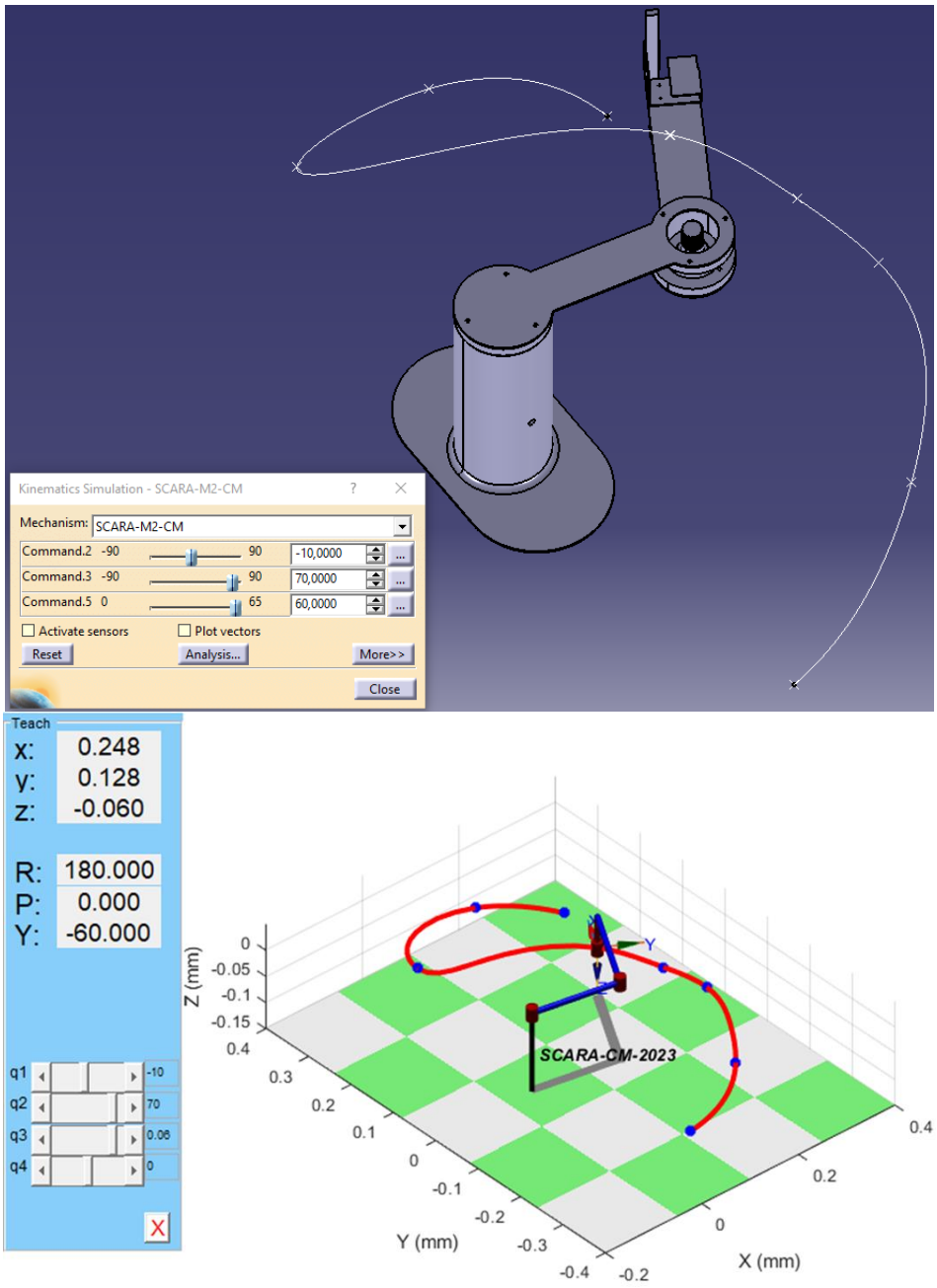

Figure IV. 28 Fifth waypoint position with CATIA V5 and Matlab

In (Figure IV.29) displays the position of the robot changes to the sixth point Px=0mm, Py=270mm, Pz=-59mm at time 3.9660 s, with the first joint at an angle of 50 degrees, the second joint at a 75 degree angle, and the third joint at d3=59 mm

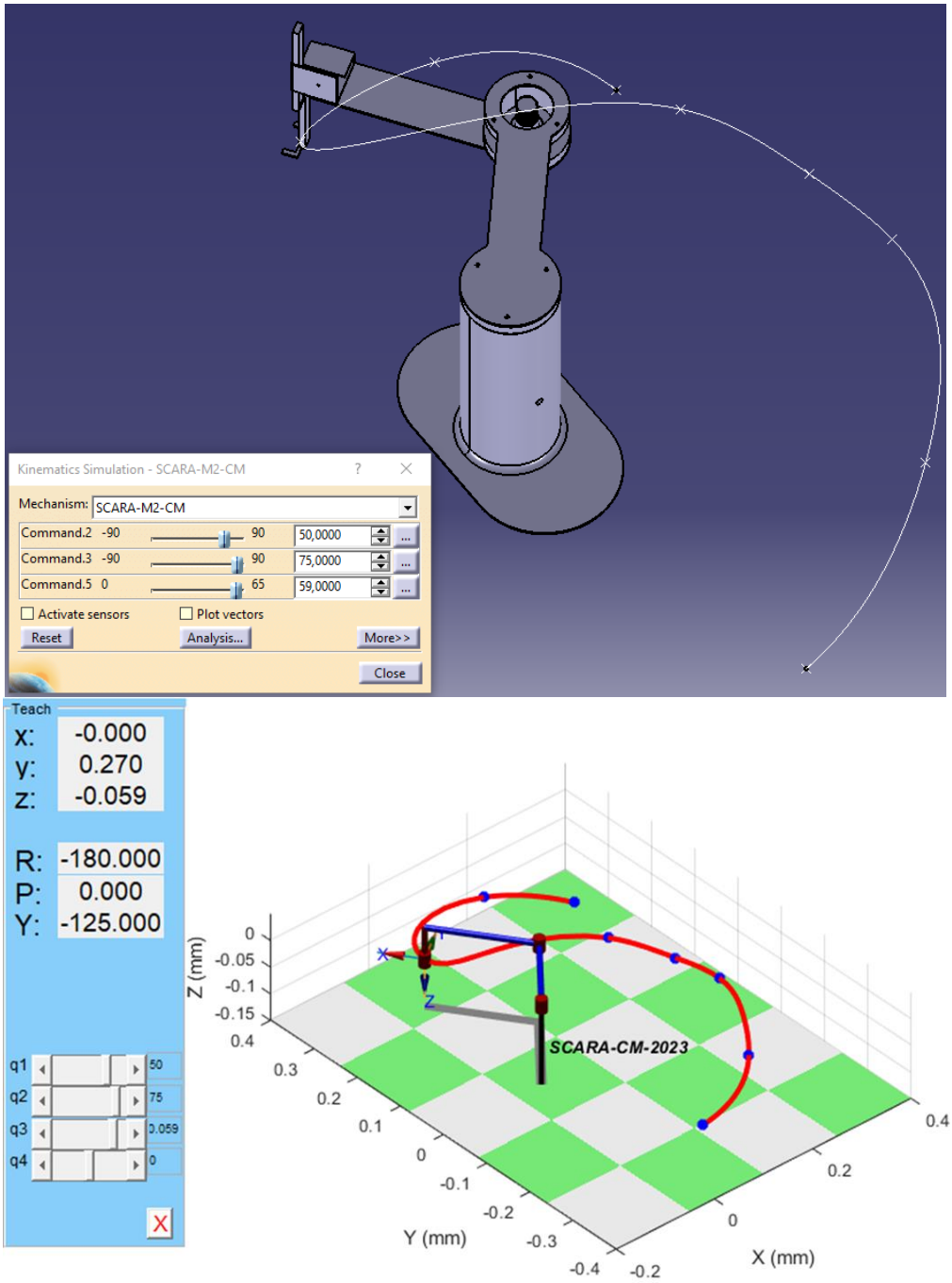

Figure IV. 29 Sexth waypoint position with CATIA V5 and Matlab

The robot's location is shown changing to the seventh point in (Figure IV.30), where Px=138mm, Py=291mm, and Pz=-20mm are the new coordinates at time 4.6650 s. The first joint is at an angle of 45 degrees, the second joint is at a 37 degree angle, and the third joint is at d3=20 mm.

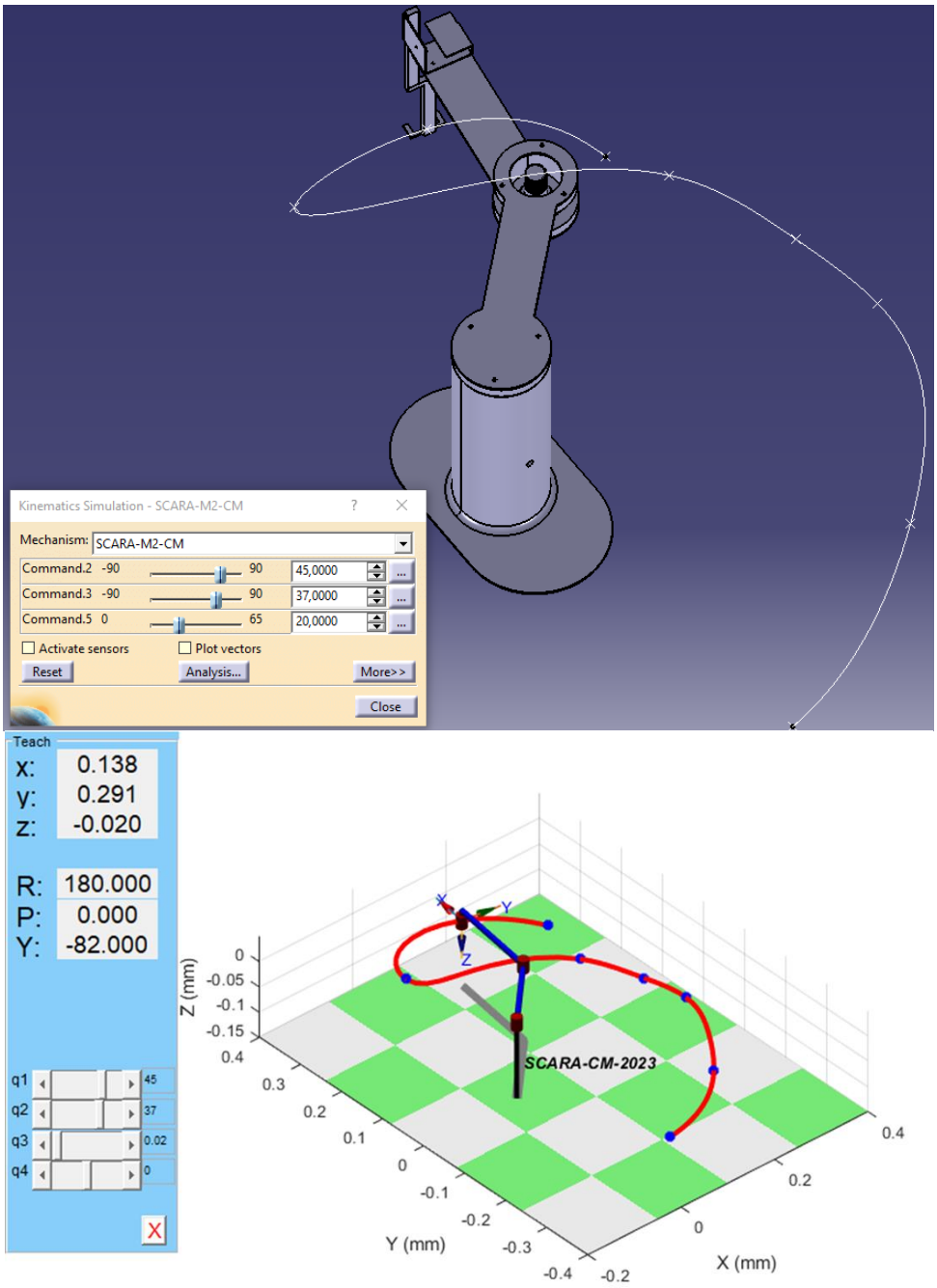

Figure IV. 30 Seventh waypoint position with CATIA V5 and Matlab

Our robot is shown in (Figure IV.31) at its final position, which is Px=234 mm, Py=191 mm, and Pz=-21 mm at time 5.200 s, with the first joint at a 10 degree angle, the second joint at a 55 degree angle, and the third joint at d3=21 mm. While CATIA was used to create the first figure, Matlab was used to make the second.

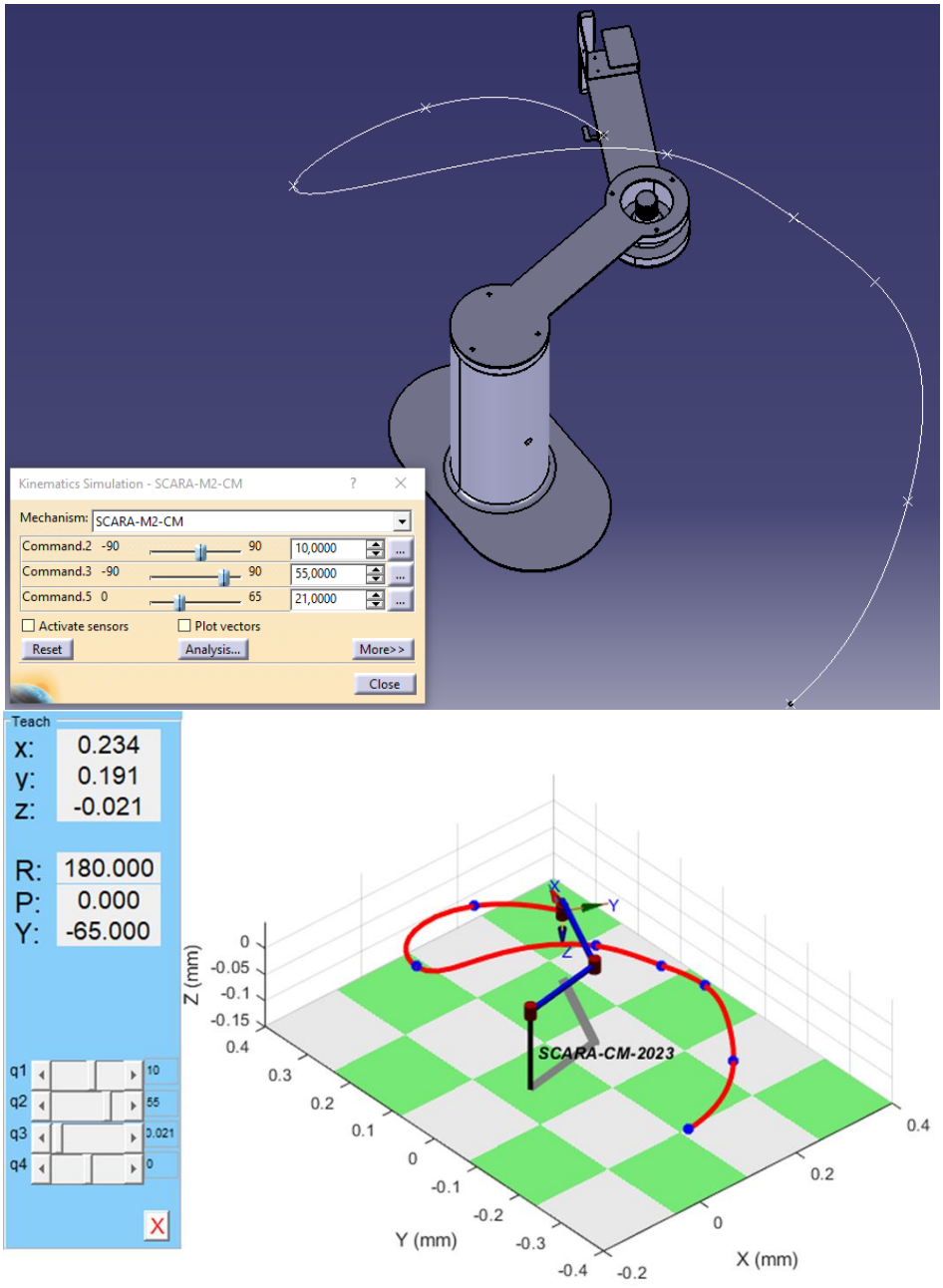

Figure IV. 31 Eighth waypoint position with CATIA V5 and Matlab

We have considered our SCARA robot with these four joints, shown in (Figure IV.16). The Denavit-Hartenberg parameters are given in (Table IV.7). The passage nodes representing the task assigned to the robot are given in (Table IV.8). The robot is initially at rest, and comes to a complete stop at the end of the trajectory. According to the graphs obtained with Matlab and CATIA V5, we can see that we have achieved the same results. (Figures IV.24- IV.31) show the comparison of trajectories in the operational space of the RRPR robot.

IV.6 Conclusion

The objective of this chapter was to make a presentation of the mechanical part of our robot, with exposure to different steps of its design and its realization. To achieve this, we started by designing with CATIA V5, then simulation with CATIA V5 and Matlab, and then manufacturing the parts.

We can conclude from comparing the outputs of the two software that our robot was capable of passing through the eight positions in the path while has not exceeded its maximum geometric constraints and it reaches the values $\theta_{1_{Max}}$ = 90 deg, $\theta_{2_{Max}}$= 87.8399 deg and $d_{3_{Max}}$= 65 mm.

GENERAL CONCLUSION

General conclusion

It is shown in this thesis that the objective of designing and constructing the RRPR Scara robot has been achieved, and this design is analyzed with CATIA V5 and Matlab.

In this work, we took advantage of the different mathematical modeling approaches, knowing that was the most important part of the robotics field, we started with geometric modelling began with direct geometric modeling, which enabled us to find the location of the terminal organ in the base frame as a function of the joint variables of the mechanism. Geometry, which gave us the articular variables as a function of Cartesian variables, followed by direct kinematics to obtain the speed terminal organ velocity as a function of joint velocities.

Our project allowed us to deepen our theoretical and practical knowledge in the field of robots, both in terms of mechanics and electronics, and this dissertation has enabled us to learn how to manage a project from start to finish, and to put into practice the knowledge acquired throughout our university training.

For future tasks, it is intended to change servo motors ±90° to stepper motors ±180° for more precision. We will also improve the control of our robot by giving it coordinates of points in space and controlling the travel speed. We also want to create a terminal organ that will make it simpler to assemble and disassemble several tools for different tasks.

APPENDIX

TECHNICAL DRAWINGS OF SCARA ROBOT PARTS

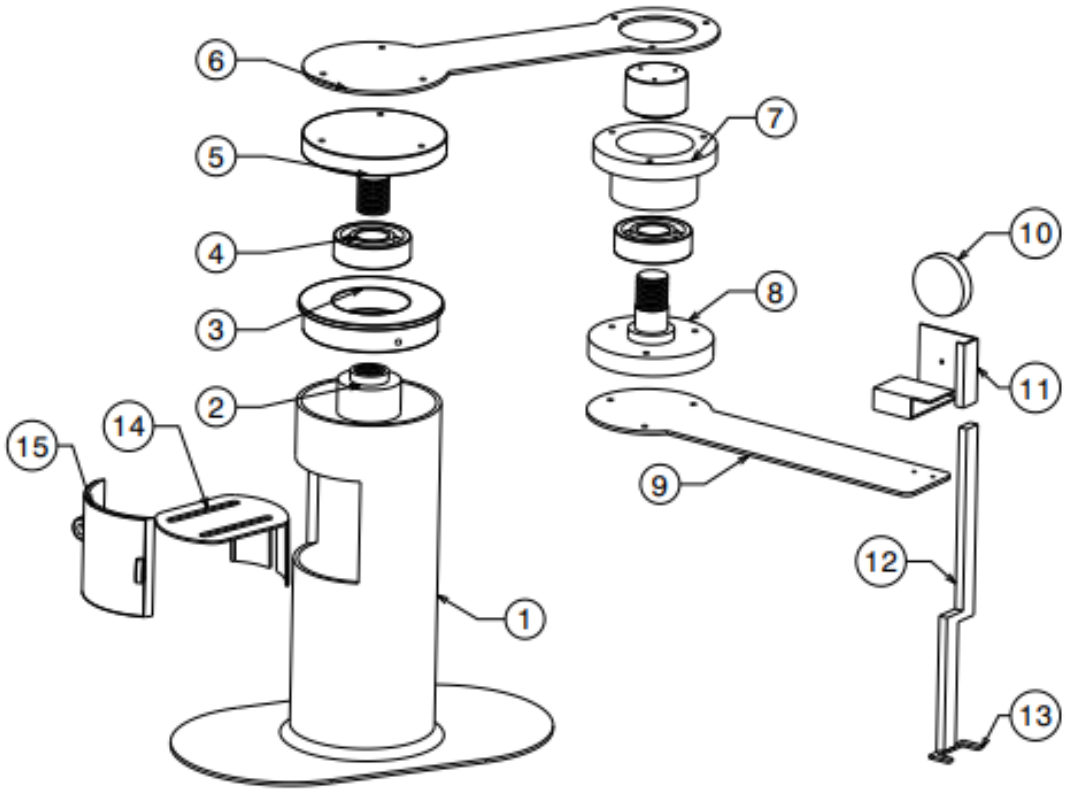

N	PARTS	Quantity
01	BODY	01
02	NUT	02
03	BEARING HOUSING I	01
04	BEARING	02
05	ROD BERING I	01
06	ARM I	01
07	BEARING HOUSING II	01
08	ROD BERING II	01
09	ARM II	01
10	PINION	01
11	RANCK AND PINION SUPORT	01
12	RANCK	01
13	TERMINAL ORGAN	01
14	SERVO MOTOR SUPORT	01
15	DOOR	01

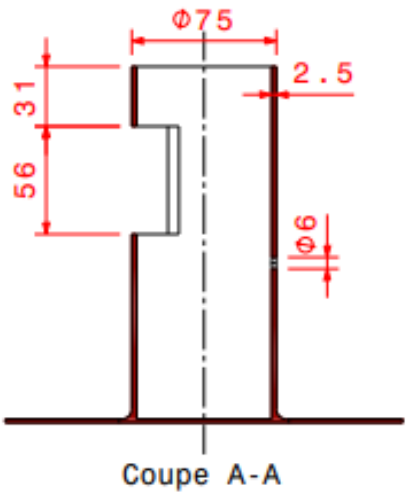

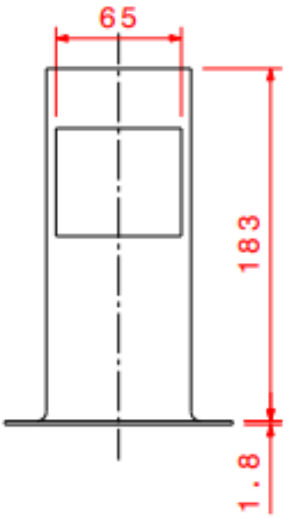

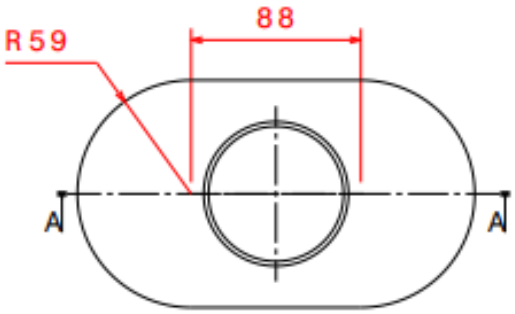

SCARA ROBOT RRPR		QUANTITY: 01	N°: M2/GM/CM		UNYVERSITY OF DJILALI BOUNAAMA	
DRAWN BY : B.S - BA	25/05/2023	TITEL: BODY				
VERIFIED BY : B.N	25/05/2023					
APPROVED BY : B.N	04/06/2023	MATERIAL: steel	WEIGHT: 1200g	SCALE: 1:3	SIZE: A4	

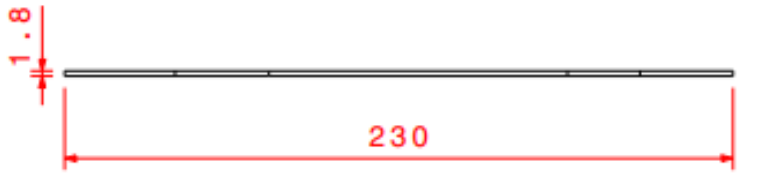

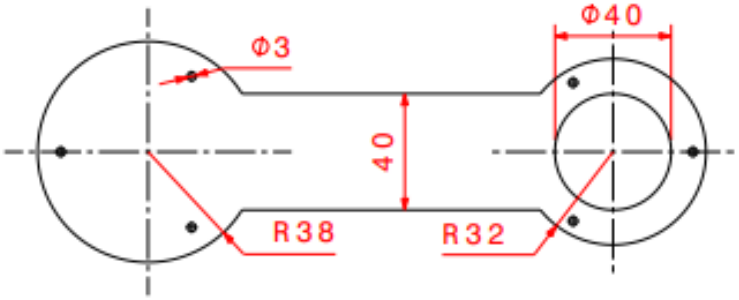

SCARA ROBOT RRPR		QUANTITY: 01	N°: M2/GM/CM		UNYVERSITY OF DJILALI BOUNAAMA	
DRAWN BY : B.S - BA	25/05/2023	TITEL: ARM I				
VERIFIED BY : B.N	25/05/2023					
APPROVED BY : B.N	04/06/2023	MATERIAL: Galvanized Steel	WEIGHT: 100g	SCALE: 1:2	SIZE: A4	

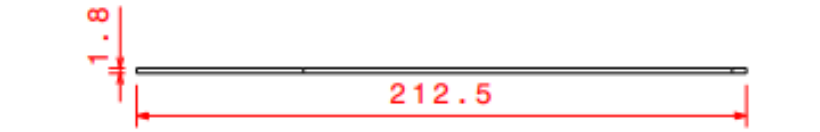

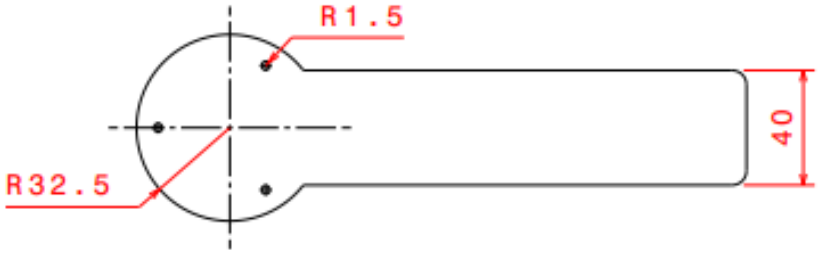

SCARA ROBOT RRPR		QUANTITY: 01	N°: M2/GM/CM		UNYVERSITY OF DJILALI BOUNAAMA	
DRAWN BY : B.S - BA	25/05/2023	TITEL: ARM II				
VERIFIED BY : B.N	25/05/2023					
APPROVED BY : B.N	04/06/2023	MATERIAL: Galvanized Steel	WEIGHT: 100g	SCALE: 1:2	SIZE: A4	

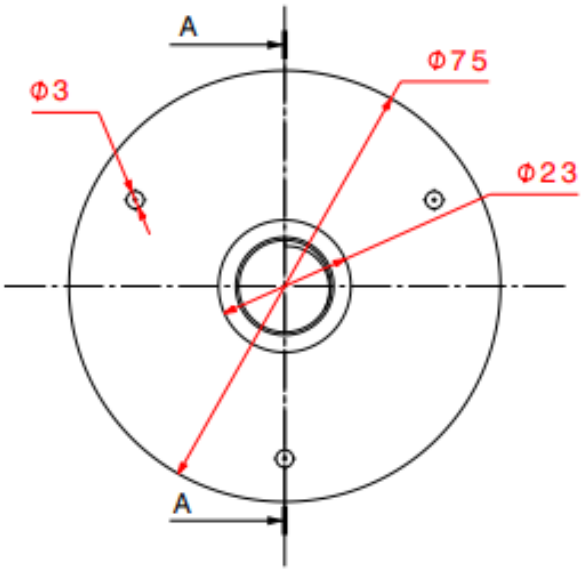

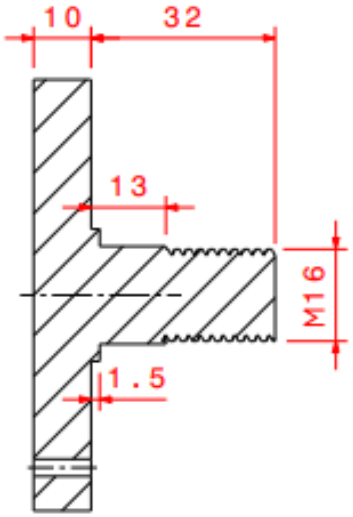

Coupe A-A

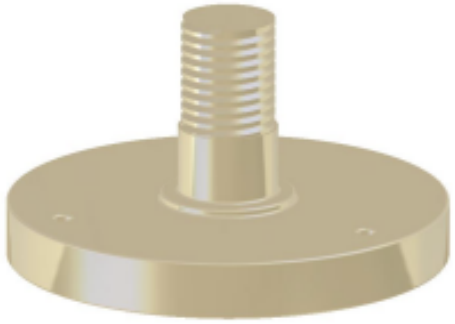

SCARA ROBOT RRPR		QUANTITY: 01	N°: M2/GM/CM		UNYVERSITY OF DJILALI BOUNAAMA	
DRAWN BY : B.S - BA	25/05/2023	TITEL: ROD BEARING I				
VERIFIED BY : B.N	25/05/2023					
APPROVED BY : B.N	04/06/2023	MATERIAL: Plastic	WEIGHT: 90g	SCALE: 1:1	SIZE: A4	

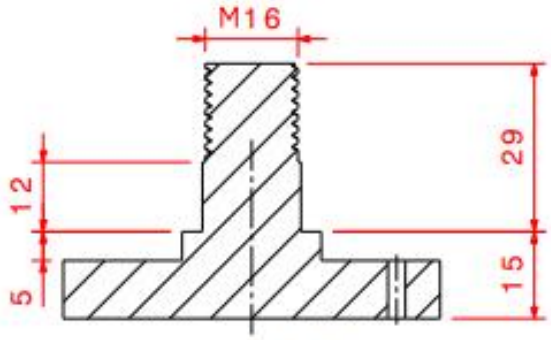

Coupe A-A

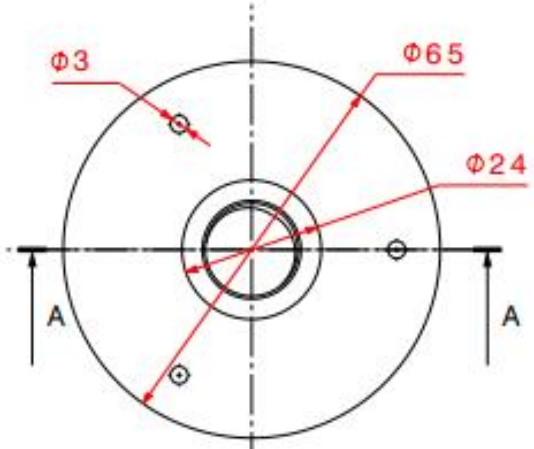

SCARA ROBOT RRPR		QUANTITY: 01	N°: M2/GM/CM		UNYVERSITY OF DJILALI BOUNAAMA	
DRAWN BY : B.S - BA	25/05/2023	TITEL: ROD BEARING II				
VERIFIED BY : B.N	25/05/2023					
APPROVED BY : B.N	04/06/2023	MATERIAL: Plastic	WEIGHT: 91g	SCALE: 1:1	SIZE: A4	

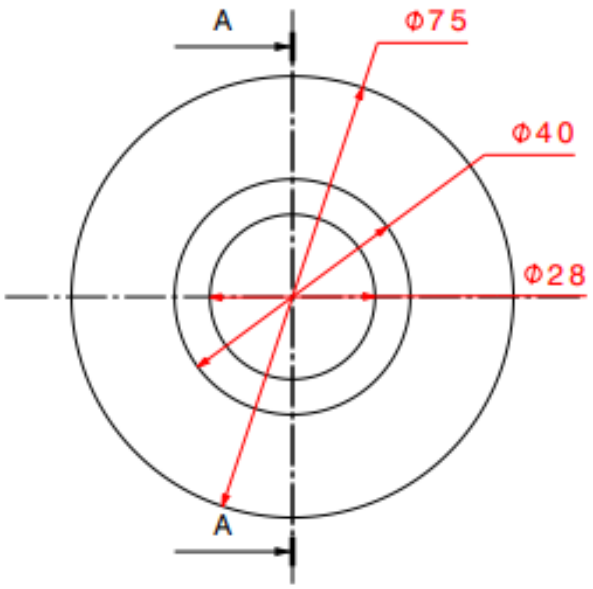

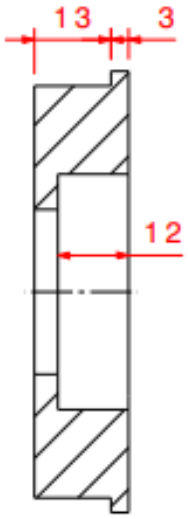

Coupe A-A

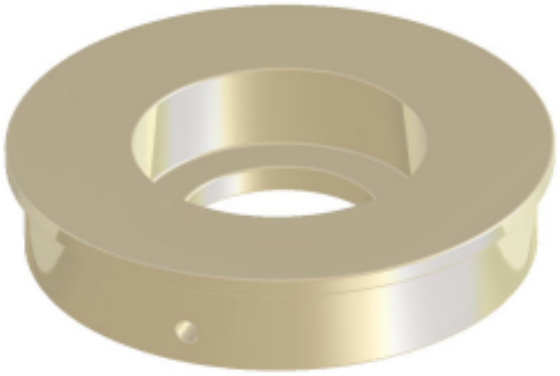

SCARA ROBOT RRPR		QUANTITY: 01	N°: M2/GM/CM		UNYVERSITY OF DJILALI BOUNAAMA	
DRAWN BY : B.S - BA	25/05/2023	TITEL: BEARING HOUSING I				
VERIFIED BY : B.N	25/05/2023					
APPROVED BY : B.N	04/06/2023	MATERIAL: Plastic	WEIGHT: 93g	SCALE: 2:1	SIZE: A4	

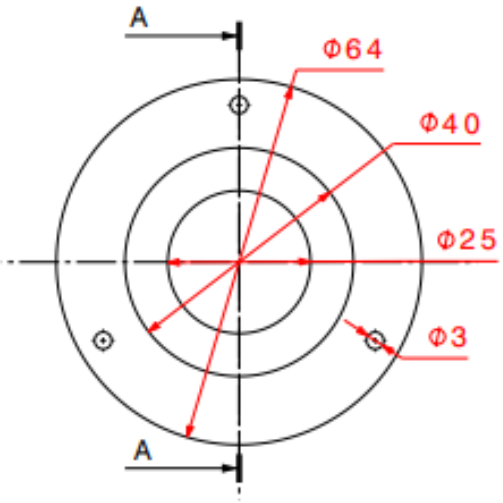

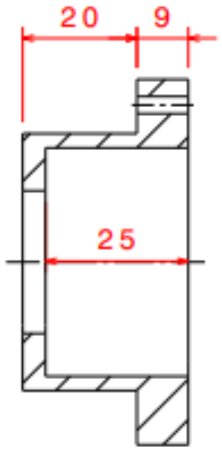

Coupe A-A

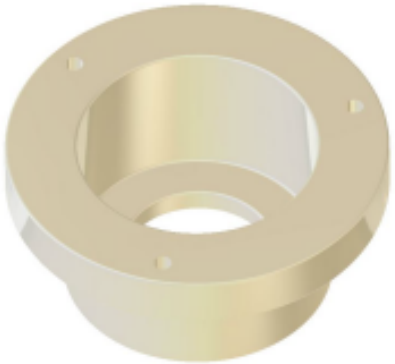

SCARA ROBOT RRPR		QUANTITY: 01	N°: M2/GM/CM		UNYVERSITY OF DJILALI BOUNAAMA	
DRAWN BY : B.S - BA	25/05/2023	TITEL: BEARING HOUSING II				
VERIFIED BY : B.N	25/05/2023					
APPROVED BY : B.N	04/06/2023	MATERIAL: Plastic	WEIGHT: 92g	SCALE: 1:1	SIZE: A4	

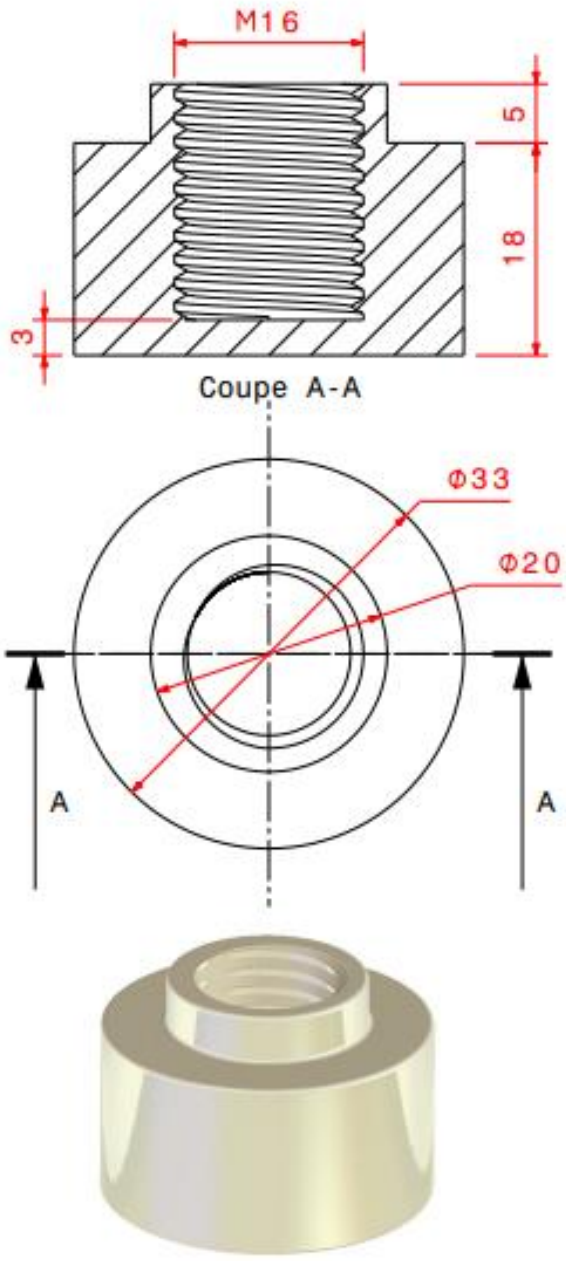

SCARA ROBOT RRPR		QUANTITY: 01	N°: M2/GM/CM		UNYVERSITY OF DJILALI BOUNAAMA	
DRAWN BY : B.S - BA	25/05/2023	TITEL: NUT I				
VERIFIED BY : B.N	25/05/2023					
APPROVED BY : B.N	04/06/2023	MATERIAL: Plastic	WEIGHT: 30g	SCALE: 2:1	SIZE: A4	

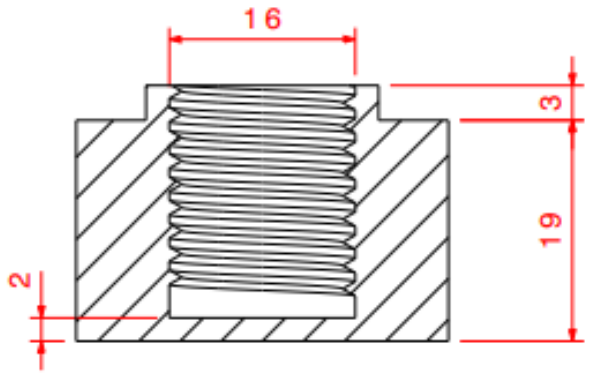

Coupe A-A

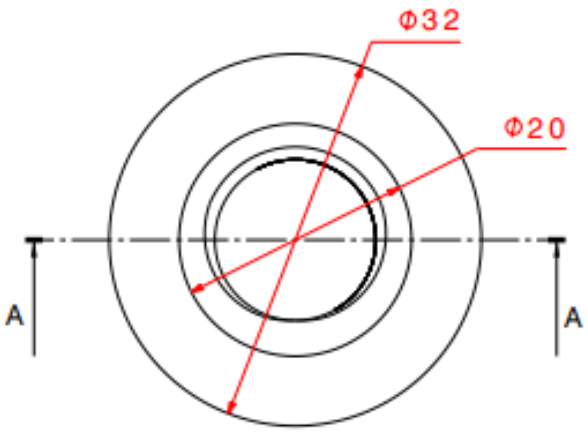

SCARA ROBOT RRPR		QUANTITY: 01	N°: M2/GM/CM		UNYVERSITY OF DJILALI BOUNAAMA	
DRAWN BY : B.S - BA	25/05/2023	TITEL: NUT II				
VERIFIED BY : B.N	25/05/2023					
APPROVED BY : B.N	04/06/2023	MATERIAL: Plastic	WEIGHT: 30g	SCALE: 2:1	SIZE: A4	

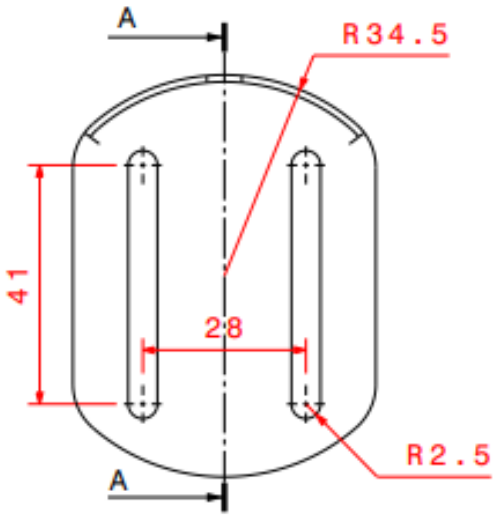

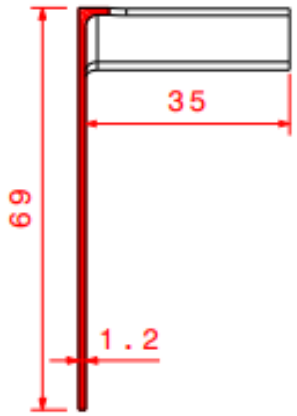

Coupe A-A

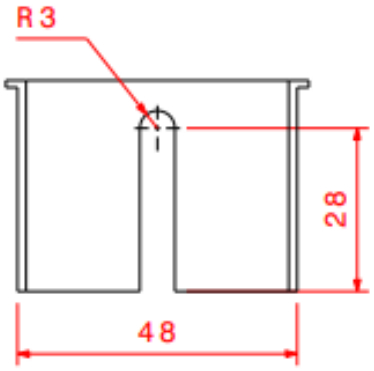

SCARA ROBOT RRPR		QUANTITY: 01	N°: M2/GM/CM		UNYVERSITY OF DJILALI BOUNAAMA	
DRAWN BY : B.S - BA	25/05/2023	TITEL: MOTOR SUPPORT				
VERIFIED BY : B.N	25/05/2023					
APPROVED BY : B.N	04/06/2023	MATERIAL: Steel	WEIGHT: 210g	SCALE: 1:1	SIZE: A4	

ARDUINO PROGRAM

```
#include <SoftwareSerial.h>

#include <Servo.h>

#define BT_RX 0

#define BT_TX 1

SoftwareSerial bluetooth(BT_RX, BT_TX); // RX, TX

Servo servo1;

Servo servo2;

Servo servo3;

Servo servo4;

void setup() {

  bluetooth.begin(9600);

  servo1.attach(8);

  servo2.attach(9);

  servo3.attach(10);

  servo4.attach(11);

}

void loop() {

  if (bluetooth.available()) {

    char command = bluetooth.read();

    if (command == '1') {

      int angle = bluetooth.parseInt();
```

```
      servo1.write(angle);
    } else if (command == '2') {
      int angle = bluetooth.parseInt();
      servo2.write(angle);
    } else if (command == '3') {
      int angle = bluetooth.parseInt();
      servo3.write(angle);
    } else if (command == '4') {
      int angle = bluetooth.parseInt();
      servo4.write(angle);
    }
  }
}
```

REFERENCES

[1] Zhang, Yunong, and Long Jin. Robot manipulator redundancy resolution. John Wiley & Sons, 2017.

[2] Noshahi, Sara Fatima, et al. "Design and fabrication of an affordable scara 4-dof robotic manipulator for pick and place objects." 2019 14th International Joint Symposium on Artificial Intelligence and Natural Language Processing (iSAI-NLP). IEEE, 2019.

[3] BOUMAHDI, Mouloud. "Conception et analyse d'un robot SCARA." (2019).

[4] Urrea, Claudio, and John Kern. "Modeling, simulation and control of a redundant SCARA-type manipulator robot." International Journal of Advanced Robotic Systems 9.2 (2012): 58.

[5] Lewis, Frank L., Darren M. Dawson, and Chaouki T. Abdallah. Robot manipulator control: theory and practice. CRC Press, 2003.

[6] Elhafnaoui, et al. "commande et realisation d un robot scara a 4 degre de liberte." (2022).

[7] Siciliano, Bruno, et al. "Robotics: Modelling, Planning and Control" (2009)

[8] DEMİRCİ, Alper Erdem. Design and analysis of a scara robot. Diss. DEÜ Fen Bilimleri Enstitüsü, 2013.

[9] Dombre, E. "Analyse et modélisation des robots manipulateurs, 2ème éd." France: Hermès Sciences (2001).

[10] https://www.engineering.com/story/how-to-choose-between-delta-vs-scara-robots

[11] https://www.controlsdrivesautomation.com/Force-controlled-parallel-robot

[12] Kelly, Rafael, Victor Santibáñez Davila, and Julio Antonio Loría Perez. Control of robot manipulators in joint space. Springer Science & Business Media, 2005.

[13] SOLTANI, Amir, and Nadir BENDALI. "Etude du mouvement optimal d'un bras manipulateur à 3 degrés de liberté en exécutant des taches imposées." (2021).

[14] Khalil, Wisama, and Etienne Dombre. Modeling identification and control of robots. CRC Press, 2002.

[15] John, J. Craig. "Introduction to robotics: mechanics and control." Reading: Addison-Wesley (1989).

[16] Spong, Mark W., Seth Hutchinson, and Mathukumalli Vidyasagar. Robot modeling and control. Vol. 3. New York: Wiley, 2006

[17] Rodd, Michael G. "Introduction to robotics: Mechanics and control: John J. Craig." (1987)

[18] Tickoo, Sham. CATIA V5-6R2018 for Designers. Cadcim Technologies, 2018.

[19] https://www.brainkart.com/article/Assembly-modeling_5721/

[20] https://www.teslamechanicaldesigns.com

[21] Chevalier, André. Guide du dessinateur industriel. Hachette, 2005.

[22] https://www.ggbearings.com/en/why-choose-ggb

[23] https://www.britannica.com/technology/differential-gear

[24] https://www.electrical4u.com/what-is-servo-motor

[25] https://www.arduino.cc

[26] Iqbal, Md Rashed, Umme Aysha, and Tanjila Robyat. 5 degree of freedom robotic Arm. Diss. BRAC University, 2016

[27] https://www.wiltronics.com.au/wiltronics-knowledge-base/what-are-jumper-wires

[28] https://maker.pro/breadboard/tutorial/an-introduction-to-breadboards-and-their-uses

[30] Tinkercad.com